

EDWARD P.J. PARROTT  
CHINESE UNIVERSITY OF HONG KONG, DEPARTMENT OF ELECTRONIC ENGINEERING,  
SHATIN, NEW TERRITORIES, HONG KONG SAR, CHINA

J. AXEL ZEITLER\*  
UNIVERSITY OF CAMBRIDGE, DEPARTMENT OF CHEMICAL ENGINEERING AND  
BIOTECHNOLOGY, NEW MUSEUMS SITE, PEMBROKE STREET,  
CAMBRIDGE CB2 3RA, UNITED KINGDOM

# Terahertz Time-Domain and Low-Frequency Raman Spectroscopy of Organic Materials

With the ongoing proliferation of terahertz time-domain instrumentation from semiconductor physics into applied spectroscopy over the past decade, measurements at terahertz frequencies ( $1 \text{ THz} = 10^{12} \text{ Hz} = 33 \text{ cm}^{-1}$ ) have attracted a sustained growing interest, in particular the investigation of hydrogen-bonding interactions in organic materials. More recently, the availability of Raman spectrometers that are readily able to measure in the equivalent spectral region very close to the elastic scattering background has also grown significantly. This development has led to renewed efforts in performing spectroscopy at the interface between dielectric relaxation phenomena and vibrational spectroscopy. In this review, we briefly outline the underlying technology, the physical phenomena governing the light–matter interaction at terahertz frequencies, recent examples of spectroscopic studies, and the current state of the art in assigning spectral features to vibrational modes based on computational techniques.

Index Headings: **Terahertz time-domain spectroscopy; Low-frequency Raman spectroscopy; Organic materials; Crystalline structure; Amorphous structure; Computational methods.**

## INTRODUCTION

In the past decade, terahertz time-domain spectroscopy (THz-TDS) has emerged as a very attractive technique used to perform vibrational spectroscopy at frequencies spanning from 100 GHz to 3 THz ( $3\text{--}100 \text{ cm}^{-1}$ ). A search performed across numerous databases indicates a surge of interest in the pursuit of spectroscopy in the low-frequency end of the far-infrared (far-IR) region of the electromagnetic spectrum (Fig. 1). Spectroscopy at terahertz frequencies is often referred to as far-IR or submillimeter spectroscopy<sup>1,2</sup> (Fig. 1), and this has been a very active field of research, in particular from the 1960s onward. In the 1960s, the breakthrough for far-IR spectroscopy came with the development of numerical Fourier transformation techniques together with the emerging availability of digital computers, which for the first time allowed the use of Michelson interferometers for routine spectroscopy applications.<sup>3</sup> Likewise the development of ultrafast optics and semiconductor physics has made THz-TDS technology possible. Today terahertz spectroscopy is readily accessible to a much larger number of research groups, and this is reflected in the breadth and quantity of recent spectroscopic

investigations. Spectroscopy into the properties of organic molecular crystals has been a field of particular interest in this context because the low photon energy at terahertz frequencies makes it possible to excite intermolecular motions using THz-TDS. This has been exploited in numerous studies in the field of solid-state characterization of several hydrogen-bonded crystallographic structures, such as polymorphism, cocrystals, hydrates, and solvates. Apart from applications in hydrogen-bonded crystals, a number of exciting applications characterizing polar liquids have sparked renewed interest in the spectroscopy community.

At the same time, the improvements in notch-filter technology and in the stability and wavelength specificity of diode lasers over the past decade have resulted in the availability of new Raman spectrometers, able to reliably access the terahertz region. Known as low-frequency Raman, ultra-low-frequency Raman, Rayleigh-wing, or THz-Raman spectroscopy, this relatively new field presents a complementary tool to THz-TDS for studying the low-frequency interactions in materials, in particular the low-frequency motions attributed to crystalline order. This more robust and affordable technology (compared to the previously used low-frequency Raman spectrometers, mainly based on double- or triple-grating technology) has also triggered a surge in the Raman field somewhat similar to the introduction of THz-TDS in the infrared (IR) area.

\* Author to whom correspondence should be sent. E-mail: jaz22@cam.ac.uk.

DOI: 10.1366/14-07707

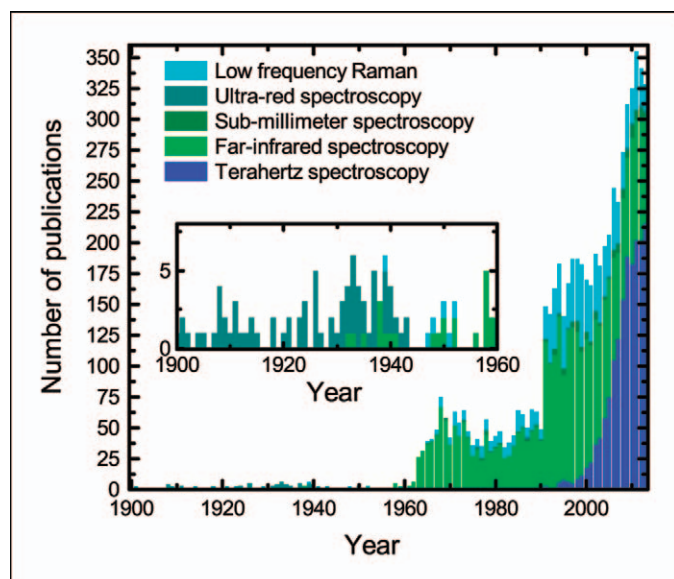


**Fig. 1.** Research activity in spectroscopy at terahertz frequencies as measured by the publication output of peer-reviewed research papers in the period 1900–2013 and classified by terminology used to describe the technique.

The assignment of the spectral features to vibrational modes is more complex at terahertz frequencies than at the mid-IR (for both THz-TDS and Raman measurements) because the periodic nature of the crystal structure also needs to be taken into account, given that, depending on the flexibility of the studied molecules, mixing between inter- and intramolecular modes takes place. In addition, for Raman spectroscopy even more computationally intense calculations are required to determine the Raman intensities of these modes. This results in different subsets of the calculated modes being either IR active or Raman active, due to their differing selection rules.

Although there have been distinct difficulties in performing spectroscopy at terahertz frequencies, there is at least one important distinction that is unique to spectroscopy at terahertz frequencies compared to vibrational spectroscopy at higher frequencies:  $h\nu$  relative to  $kT$  (where  $h$  is Planck's constant and  $k$  is Boltzmann's constant) have very different relative ratios at terahertz frequencies than at the mid-IR. At room temperature,  $kT$  is approximately 6 THz. Above 12 THz, there are hardly any excited states present at room temperature, and only about 10% of such states are observed at 12 THz. However, in the frequency range that can be accessed using THz-TDS (typically up to 3–4 THz), there is a significant population of excited states, leading to a broadening of the observed vibrational modes and dramatic changes in the spectra upon cooling to below room temperature.

In this review, we limit our discussion to the spectroscopy of organic hydrogen-bonding molecules; for a more detailed overview of the wide range of other applications of terahertz spectroscopy, the reader is

referred to the more specialist literature.<sup>4–18</sup> We also highlight that spectroscopy at terahertz frequencies has a much longer tradition than we can possibly cover in this review article. In the spirit of Felix Franks' comments regarding the value of "old literature",<sup>19</sup> we point out references that provide good summaries of previous work throughout this review. However, such an endeavor is almost inevitably going to fall short of our aspirations, and we emphasize that the references presented here will serve as a useful starting point but are incomplete.

## TECHNIQUES

**Terahertz Time-Domain Spectroscopy.** Modern THz-TDS owes its beginnings to the pioneering work of Auston on the picosecond gating of semiconductor devices using optical pulses to control a switch.<sup>20</sup> Initially these gated switches were confined to the transmission of pulses along transmission lines, but it was noted that they also acted as photoconductive (PC) transmitters and detectors. First, millimeter wave pulses<sup>21</sup> and, then, terahertz pulses<sup>22,23</sup> were developed by groups headed by Auston and Grischkowsky.<sup>24,25</sup> These optically gated antenna structures provided a new way to access the "terahertz gap" region, thanks to the development of ultrafast, femtosecond near-infrared (NIR) lasers. Right at the onset of this research, the spectroscopic applications were already being highlighted by Grischkowsky and coworkers in early work on characterizing semiconductor substrates, observing the rotational lines of a number of gases and measuring the spectra of flames.<sup>26–29</sup>

Aside from PC generation and detection, another technique commonly employed in THz-TDS is electro-optic (EO) generation and detection. First demonstrated for femtosecond electrical transients by Auston and Nuss,<sup>30</sup> the technique was simultaneously demonstrated for the detection of free-space transients by three independent groups.<sup>31–33</sup> Electro-optic generation uses the Pockels' effect, where an incident electric field (in this case, the terahertz transient) produces a birefringence in a crystal such as zinc telluride (ZnTe) or gallium phosphide (GaP), thus rotating the phase of the probe laser pulse. Measurement of the relative polarization of the pulse retrieves the magnitude and phase of the terahertz electric field. Advantages over PC techniques include a flat frequency response and the researchers' ability to extend the measured range, with a 7 THz band width reported for a GaP detector.<sup>34</sup> Terahertz time-domain spectroscopy measurements can be performed in both transmission and reflection modalities; however, at present the majority of spectroscopic studies have used the transmission mode. This has the advantage of ensuring that the bulk spectroscopic properties of the material are measured. The basic transmission THz-TDS setup is shown in Fig. 2A. The detector is biased by a square wave potential derived from the reference oscillator of a lock-in amplifier, which receives and extracts the modulated detector signal, in this case from the current registered

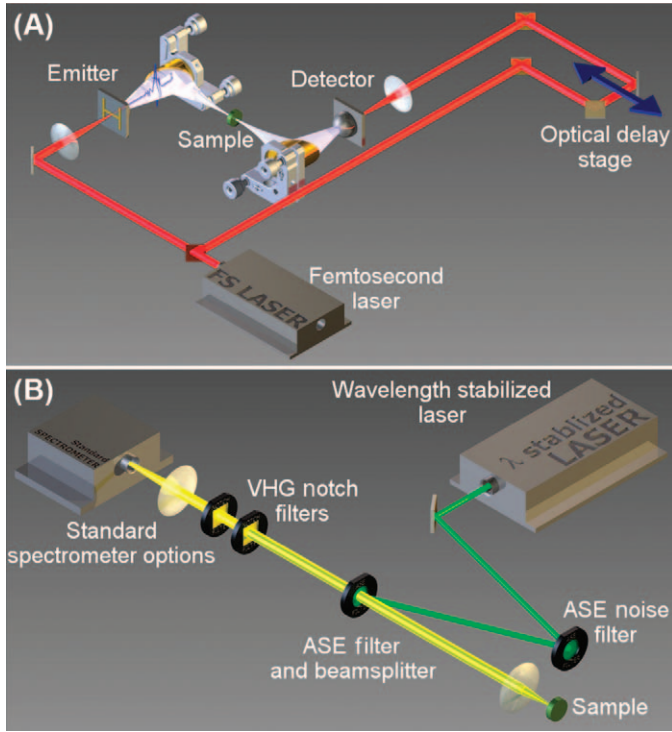


**Fig. 2. Basic spectroscopy experimental setups. (A) Terahertz time-domain spectroscopy. (B) Raman spectroscopy.**

by a PC antenna. In addition, the femtosecond laser pulses act as an optical gate, ensuring that the detector is active only for a short time, depending on the femtosecond laser pulse width. This and the use of lock-in techniques result in signal-to-noise ratios (SNRs) greater than  $10^4$ .<sup>27</sup> However, to measure the full time-domain terahertz pulse, the optical delay must be altered between the pump emission laser pulse and the probe detection laser pulse. By systematically measuring a number of points, researchers record the terahertz time-varying electric field, from which the common step is to recover the frequency-dependent amplitude and phase information through the use of a Fourier transform. For further information and insights into the techniques of THz-TDS, the reader is directed to other sources.<sup>4,9</sup>

In THz-TDS, complex dielectric loss spectra can be calculated directly from the experimental data at terahertz frequencies because it can be used to measure the amplitude and phase of the transmitted waveform, thereby allowing the complex refractive index to be calculated. The complex refractive index  $\hat{n}(\omega)$  can be described in terms of the real part of the refractive index  $n(\omega)$  and its imaginary part, the index of absorption  $\kappa(\omega)$  (also sometimes called the extinction coefficient):

$$\hat{n}(\omega) = n + i\kappa \quad (1)$$

Using the speed of light in vacuum  $c$  and the angular frequency  $\omega$  ( $= 2\pi\nu$ ), the absorption coefficient can be

extracted from the index of absorption:

$$\alpha(\omega) = \frac{2\omega\kappa(\omega)}{c} \quad (2)$$

This complex refractive index can be expressed in terms of the dielectric losses ( $\hat{\epsilon}$ ):

$$\hat{\epsilon}(\omega) = \epsilon'(\omega) - i\epsilon''(\omega) = \hat{n}(\omega)^2 \quad (3)$$

where  $\epsilon'$  is the real and  $\epsilon''$  the imaginary part of the dielectric losses. It is, hence, possible to convert between the absorption spectra that are commonly used in IR spectroscopy and the dielectric loss spectra by using the following expressions:

$$\begin{aligned} \epsilon'(\omega) &= n(\omega)^2 - \kappa(\omega)^2 \\ \epsilon''(\omega) &= 2n(\omega)\kappa(\omega) = \frac{n(\omega)\alpha(\omega)c}{\omega} \end{aligned} \quad (4)$$

Note that the absorption coefficient in Eq. 2 can also be related to the absorbance ( $A$ ) of a material:

$$A(\omega) = -\log_e\left(\frac{I}{I_0}\right) = \alpha(\omega)d \quad (5)$$

where  $I$  is the transmitted intensity of light through a medium relative to the incident intensity  $I_0$  and  $d$  is the thickness of the medium. The absorbance makes most physical sense when written in terms of natural logarithms ( $\log_e$ ) because this results in the relationship to the absorption coefficient in Eq. 5, but some communities define the absorbance in terms of base-10 logarithms ( $\log_{10}$ ), which can give rise to confusion. Consequently, here we use either the absorption coefficient, when a thickness has been defined, or the absorption in arbitrary units, when no thickness has been calculated; in this case, absorption relates to the absorbance as defined in Eq. 5.

Further information on how to take scattering effects into account and how the optical properties can be extracted accurately from time-domain waveforms has been described in detail elsewhere.<sup>35–38</sup>

**Low-Frequency Raman Spectroscopy.** Raman spectroscopy was first observed by Raman and Krishnan in 1928 and is based on the interaction of light with the molecular vibrations and phonons of the target system.<sup>39</sup> Raman spectroscopy is similar to IR spectroscopy (and thus by extension to THz-TDS) in that both techniques measure a series of vibrational bands at different frequencies. These features are due to molecular vibrations or phonon modes of the material of interest; however, unlike IR spectroscopy, these features are sampled as a form of inelastic scattering, because they are a measurement of the transfer of energy between the molecule and the photons of the excitation laser. A Raman spectrometer (shown schematically in Fig. 2B) measures the shifts in frequency of the Raman-scattered light from a single frequency source; it is this shift in



## focal point review

frequency that corresponds to the molecular vibrations and phonon modes of the material. Since it is a scattering phenomenon, the Raman signal is intrinsically weak, especially compared to the intensity of the elastic Rayleigh-scattered light (at the source frequency), and so the spectrometer must filter out the light close to the source frequency. Traditionally the filters used for Raman spectroscopy blocked a relatively large spectral region, and so Raman shifts below  $200\text{ cm}^{-1}$  were blocked by the filters. However, the recent improvement in volumetric holographic grating notch filters and the use of stable diode lasers coupled with ultra-narrowband amplified spontaneous emission filters have resulted in the availability of affordable Raman spectrometers able to access the terahertz region.<sup>40</sup>

### MESOSCOPIC STRUCTURE AND DYNAMICS

While well-defined peaks are observed due to the long-range order present in crystalline materials, the terahertz absorption spectra of liquids and disordered solids do not exhibit any such distinctive absorption bands. The following is a brief summary of the main principles in the context of the renewed interest in spectroscopy at terahertz frequencies. In addition to the recent work using THz-TDS, over decades a large number of studies have been done using low-frequency Raman spectroscopy and far-IR spectroscopy to investigate similar effects, and we strongly recommend this literature and the references therein to the interested reader for more detailed information.<sup>41–48</sup>

**Supercooled Liquids and Glasses. Liquids.** The high-frequency wing of the dielectric loss peaks that are observed at gigahertz frequencies, and which span multiple decades of frequency, can be detected using THz-TDS. Interesting information on the intermolecular interactions in such liquids can be extracted from the analysis of the spectra.<sup>49</sup> Spectroscopy of dipole relaxation processes at terahertz frequencies goes back a long way; Poley was one of the first in 1955 to discuss the absorption at terahertz frequencies of polar liquids in the adjoining frequency regions.<sup>50</sup> He noticed an inconsistency between the extrapolated dielectric constant  $\epsilon_{\text{inf}}$  measured in the microwave region and the square of the refractive index  $n^2$  when extrapolated from measurements in the visible and IR regions, and postulated the existence of an additional region of dipolar absorption at terahertz frequencies in liquids. This has since often been referred to as Poley absorption.<sup>51</sup> These losses are mainly the result of reorientational motions of polar molecules excited by an external oscillating electric field, for example, the terahertz radiation in the case of THz-TDS (Fig. 3).<sup>52</sup> The lowest-frequency peak that dominates the spectrum in the microwave region is often referred to as the  $\alpha$  relaxation, and it represents the rotational diffusion of liquid molecules. However, the dipole relaxation processes occur on different time scales and hence can be resolved further. As mentioned before, the slow  $\alpha$

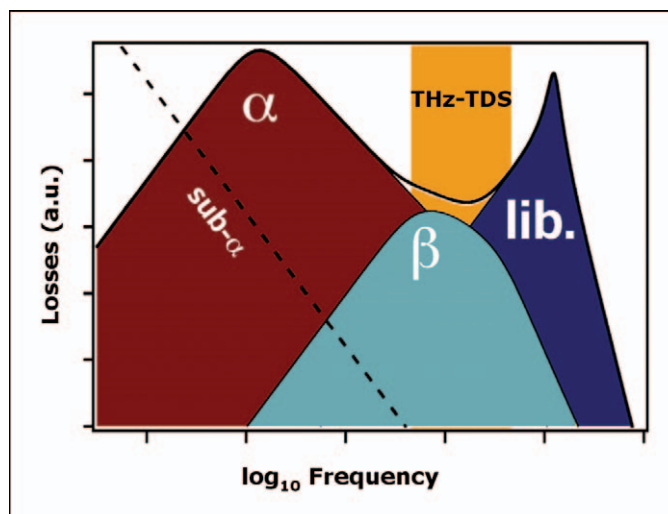


**Fig. 3.** A typical spectrum of polar liquids at terahertz frequencies (modified from Turton et al.<sup>52</sup>). Highlighted in orange is the typical range of phenomena that can be studied using current THz-TDS setups.

orientational relaxation occurs on picosecond time scales, while the fast collision-driven  $\beta$  orientational relaxation is observed on femtosecond time scales. This fast- $\beta$  relaxation process is sometimes also explained in terms of a rattling movement of molecules in the cage of their surrounding molecules within the framework of the mode-coupling theory (MCT).<sup>53</sup> Note, in this context, that the MCT is one of a number of theoretical relaxation models and, although it is widely used, it is not able to fully describe all aspects of molecular interaction. Polar, small organic molecules are known to form hydrogen-bonded chain structures; for example, the cooperative rearrangement of the alcohol–alcohol chain structure occurs on time scales of  $\approx 100$  ps, the reorientation of an individual alcohol molecule situated at the end of the alcohol–alcohol chain is faster by roughly one order of magnitude, and the relaxation of liquid molecules in the process of hydrogen-bond formation and decomposition lasts  $\approx 1$  ps.<sup>54–56</sup>

All these relaxation processes can be resolved and quantified using Debye models, such as a simple two-component model, to resolve the fast (femtosecond) and slow (picosecond) relaxation processes:

$$\hat{\epsilon}(\omega) = \epsilon_{\infty} + \frac{\Delta\epsilon_1}{1 + i\omega\tau_1} + \frac{\Delta\epsilon_2}{1 + i\omega\tau_2}. \quad (6)$$

where  $\hat{\epsilon}$  is the complex dielectric loss,  $\omega$  is the angular frequency,  $\Delta\epsilon_1$  and  $\Delta\epsilon_2$  measures the strength of the respective relaxation process, and  $\tau_1$  and  $\tau_2$  are the relaxation times. For example, in water at room temperature the two relaxation processes correspond to relaxation times of  $\tau_1 \approx 8$  ps and  $\tau_2 \approx 170$  fs. Additional Debye and oscillator terms have been added to this equation to account for molecules undergoing

hydrogen-bond formation and breaking, as well as intermolecular stretching vibrations because intermolecular stretching and libration processes were shown to contribute to the absorption of terahertz radiation by hydrogen-bonding liquids.<sup>57</sup> In general, liquids exhibit a broad absorption band in excess of the description by Debye theory, which originates from what Chantry and Gebbie termed pseudo-lattice modes and what is now more commonly referred to as the vibrational density of states (VDOS).<sup>58</sup> This effect is stronger for polar molecules than for nonpolar ones.

For a meaningful analysis of the relaxation times, it is absolutely necessary to have spectral data that spans from at least megahertz to terahertz frequencies to select the appropriate Debye model to describe the spectrum of any given liquid or liquid mixture. Without such broad spectral data, the fitting procedure becomes meaningless because all the models will fit the terahertz data alone given that it represents only the high-frequency wing of the main relaxation process. Nonetheless, once the appropriate model is known, the terahertz spectra can be used to extract unique insights into the structure and dynamics of liquids.<sup>52</sup>

A number of groups have investigated the temperature dependence of the dielectric relaxation processes in liquid water.<sup>59–63</sup> Using THz-TDS, it was possible to determine the size of the hydration shells around dissolved protons in water.<sup>60</sup> In combination with IR and molecular dynamics simulations, THz-TDS was used to study the structure of methanol–water mixtures<sup>61</sup> and acetonitrile–water mixtures.<sup>64</sup> In addition to the studies of aqueous mixtures, a number of studies have focused on the interaction between nonpolar solvents with polar solvents.<sup>65–67</sup> Recently, the dielectric response of tetramethylurea was measured using a combination of terahertz and gigahertz dielectric spectroscopies, and the measurements were compared to femtosecond IR pump–probe studies.<sup>68</sup> It was found that the dynamics of the water molecules in close vicinity to the hydrophobic urea derivative was significantly retarded but that this effect only extended approximately 12 water molecules into the bulk water phase. Yomogida and coworkers found direct evidence for a vibrational mode around 1.5 THz and an intermolecular stretching mode around 2.5 THz in measurements of a series of seven pentanol isomers.<sup>69,70</sup> (In this context, it is useful to highlight that the term *Boson peak* is sometimes used to refer to broad peaks that are centered around 1–2 THz and that have their origin in vibration-libration losses. The next section contains a more detailed discussion regarding these processes and the controversy surrounding the term *Boson peak* in this context.) Together with the dielectric relaxation data at microwave frequencies, the studies showed the complex interplay between reorientation motion and vibration dynamics in hydrogen-bonded liquids. In a separate study, Yamaguchi et al. found evidence for an intermolecular vibrational mode origi-

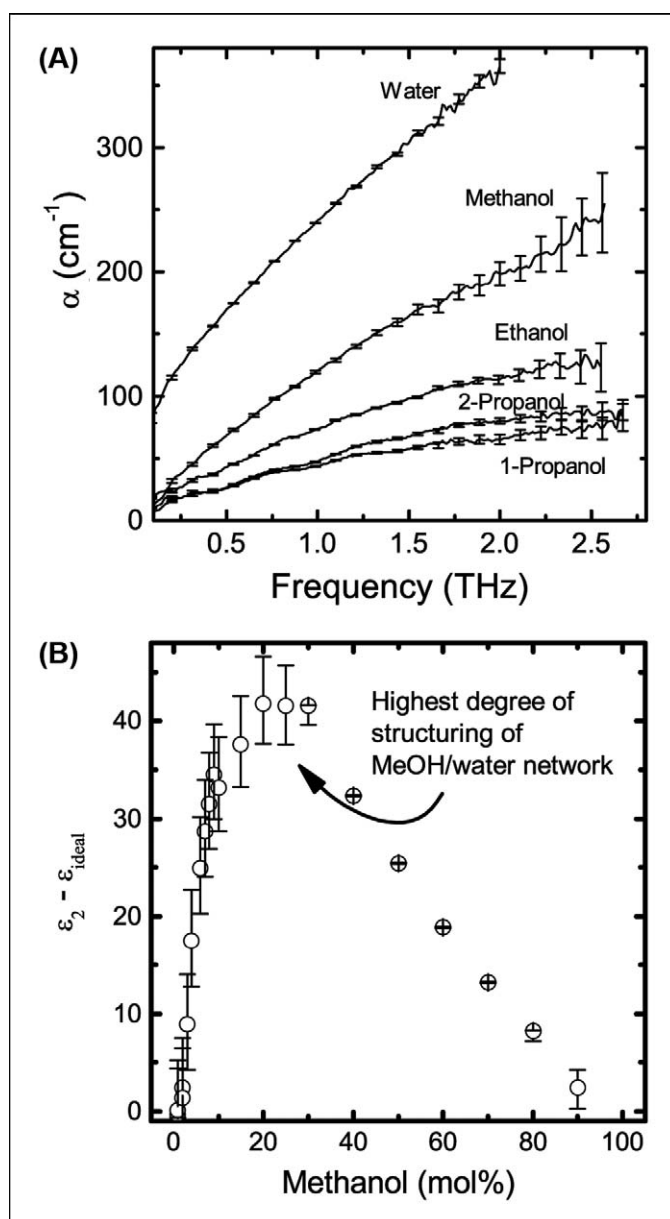


**Fig. 4.** (A) Terahertz absorption spectra of pure water and alcohols. (B) Dielectric relaxation analysis of methanol–water mixtures. The highest degree of structuring of the alcohol–water network is identified by the maximum difference between the Debye component  $\epsilon_2$  and the theoretical strength of the dielectric relaxation component for an ideal mixture,  $\epsilon_{ideal}$ . This is also the composition at which there is a minimum in the diffusivity of alcohol as measured by NMR spectroscopy (modified from Li et al.<sup>72</sup>).

nating from benzoic acid that was found to form dimers when dissolved in carbon tetrachloride.<sup>71</sup>

Terahertz spectroscopy and pulsed-field gradient NMR diffusometry have been used as complementary techniques to understand the dynamics of alcohol–water mixtures at the molecular level (Fig. 4).<sup>72</sup> The combined results showed the presence of three critical concentra-

## focal point review

tions at which a change in the dynamic regime occurs. The first is a concentration above which the intermolecular interaction between water and the alcohol hydroxyl group (–OH) becomes predominant compared to hydrophobic hydration interactions. Below this composition, the hydration shells around the hydrophobic moieties of the alcohols form predominantly, with larger hydrophobic moieties of the alcohol molecule resulting in larger hydration shells. Second, at a higher concentration, the highest degree of structuring of the hydrogen-bonded network occurs, which corresponds to the slowest translational dynamics in the mixture. Finally, at an even higher concentration the dynamics of water and alcohol molecules become increasingly independent.

While the majority of studies using THz-TDS that have been reported to date have used transmission geometry (where a thin slab of sample is confined between two windows, typically made from z-cut quartz), there have also been some very interesting developments using reflection techniques, including attenuated total reflection for such measurements.<sup>62,73–75</sup> Moller et al. provided a good review of this field.<sup>76</sup> In addition, microfluidic devices for liquid spectroscopy have also been demonstrated.<sup>77</sup>

As soon as other molecules, such as carbohydrates or proteins, are dissolved in water, it is possible to distinguish between different populations of water molecules based on the change in the relaxational dynamics because the water molecules that are part of the solvation shell exhibit a significantly different dynamics than the bulk water molecules. This concept was applied to study a wide range of molecular interactions of biomolecules during solvation: lactose;<sup>78</sup> threhalose, lactose, and glucose;<sup>79</sup> proteins;<sup>80–82</sup> protein folding;<sup>83</sup> peptides;<sup>84–86</sup> ions;<sup>87</sup> antibodies;<sup>88</sup> and urea;<sup>89</sup> among others. In addition, very interesting effects regarding the hydration of biomolecules were detected using terahertz spectroscopy,<sup>90–92</sup> including the protein dynamic transition<sup>93,94</sup> and lipid-membrane formation.<sup>95,96</sup> More detailed reviews of these topics have been published.<sup>97–101</sup> This work complemented very nicely similar studies using low-frequency Raman spectroscopy and light-scattering techniques.<sup>102–108</sup>

**Supercooled Liquids and Glasses.** Prior to the advent of THz-TDS, it was possible to measure the dielectric spectra to frequencies up to hundreds of gigahertz using interferometric techniques,<sup>109,110</sup> and the resulting spectra revealed a minimum of losses between the dielectric relaxation and far-IR resonances, as previously predicted by Wong and Angell.<sup>111</sup> However, only a limited number of experimental studies that report the spectra of supercooled liquids and glasses have been published thus far.<sup>112</sup>

Structurally, supercooled liquids and glasses are very similar to liquids, but the slower dynamics means that the terahertz spectrum becomes more strongly dominated by absorption into the VDOS that forms the libration–vibration band, or the microscopic peak, in the region of

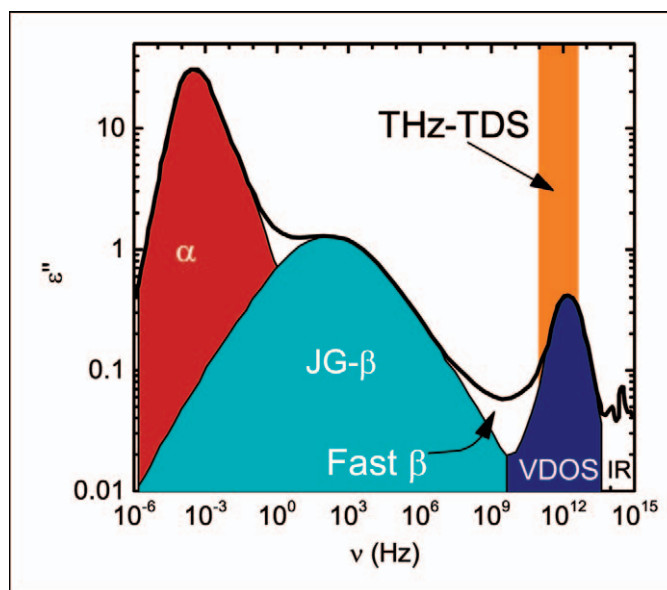


**Fig. 5.** Typical dielectric response of hydrogen-bonding disordered materials. Primary relaxation ( $\alpha$ ), Johari-Goldstein secondary relaxation (JG  $\beta$ ), MCT fast secondary relaxation (fast- $\beta$ ), VDOS peak, and intramolecular IR modes. The blue shading highlights the frequency region covered by typical THz-TDS instruments. Highlighted in orange is the typical range of phenomena that can be studied with current THz-TDS setups.

approximately 1–5 THz. In the adjacent microwave region, typically both a primary ( $\alpha$ ) and a secondary ( $\beta$ ) relaxation process can be observed, which separate in frequency as the material is cooled. As is the case for liquids, the high-frequency-loss tails of the  $\alpha$  and  $\beta$  relaxations still contribute significantly to the spectrum measured by THz-TDS (Fig. 5). Again, the primary relaxation is associated with molecular-diffusion processes, and it can no longer be measured on typical experimental time scales because the viscosity of a supercooled liquid increases at the glass transition temperature  $T_g$ .<sup>113</sup> A number of mechanisms have been proposed to explain the secondary relaxation, such as intramolecular flexibility.<sup>114</sup> However, of particular importance in the context of small organic molecules is the Johari–Goldstein (JG) secondary relaxation. The JG  $\beta$  relaxation is an actual property of disordered systems, and it was shown to exist even in glasses formed from completely rigid molecules.<sup>115</sup> Note that the JG  $\beta$  relaxation is not always clearly separated from the primary relaxation and sometimes rather forms a shoulder in the high-frequency wing of the primary relaxation peak.<sup>116</sup> It is thought that the JG  $\beta$  relaxation originates from a movement of the whole molecules and is intermolecular in nature,<sup>114,115</sup> in contrast to the intramolecular secondary relaxations that originate from movements involving only a subset of the entire molecule. Experimentally, the first absorption spectra at terahertz frequencies were acquired by means of Fourier transform infrared (FT-IR) spectroscopy from the



1960s onward. Far-infrared studies on a series of structurally and electronically different inorganic glasses showed the existence of a universal temperature-independent terahertz absorption feature that increased in intensity with frequency as  $\nu^\beta$  ( $\beta \lesssim 2$ ).<sup>117</sup> Given the frequency-squared dependence of absorption, which resembles that of a vibrational density predicted by Debye theory, it was concluded that the feature originates from disorder-induced coupling of the far-IR radiation to a density of low-frequency Debye modes. More recently, it was shown by Taraskin et al. that the VDOS of all disordered materials follows a universal frequency dependence in this spectral range, which can be resolved into two phenomena: (i) coupling to VDOS and (ii) fluctuating atomic charges in the sample.<sup>118</sup>

Reid and Evans measured the spectra of supercooled liquids and glasses of decalin solutions using far-IR spectroscopy and observed an absorption feature in the terahertz region. They referred to it as a  $\gamma$  process, following the terminology used in the dielectric spectroscopy community for the  $\alpha$  and  $\beta$  relaxation processes at lower frequencies.<sup>119</sup> Although the frequency of this  $\gamma$  process matches that of the coupling of radiation to a low-frequency Debye mode in inorganic glasses, there are two major differences between these two processes. First, the  $\gamma$  process exhibits a well-developed peak in the absorption spectra, in contrast to the Debye mode, which typically clearly resolves only when plotted as frequency-squared absorption. Second, the  $\gamma$  process is not temperature independent. The spectra clearly demonstrate the difference in temperature dependence between the relaxation processes—as the solutions are cooled, the dielectric relaxation moves from the gigahertz region to the low end of the experimentally accessible frequency window; in contrast, the  $\gamma$  process remains in the terahertz region and shifts slightly toward the higher frequencies.

It is important to clarify the term *Boson peak* because it is used somewhat inconsistently across different communities and can lead to confusion. Raman, Brillouin, and neutron-scattering studies revealed the existence of an excess in Debye density of states, commonly referred to as the Boson peak. However, in the literature the term *Boson peak* is often used for the entire peak that originates from the density of states, not only to its excess. The actual Boson peak—the excess in VDOS above the Debye level—is typically observed around 2–5 meV (0.5–1.2 THz), and its origin is still not fully understood. Although there is evidence that it can be explained by acoustic vibrations alone,<sup>120</sup> Ruffle et al. argued that, in many cases, a good agreement between theory and experiment can be achieved only by also including non-acoustic vibrational modes.<sup>121</sup> A recent study of the Boson peak in sorbitol revealed that its center frequency is around 1.1 THz and that it decreases in intensity, but does not shift in frequency, on cooling, and Ruta et al. argued that the Boson peak can be explained in terms of acoustic vibrations alone.<sup>122</sup> If this

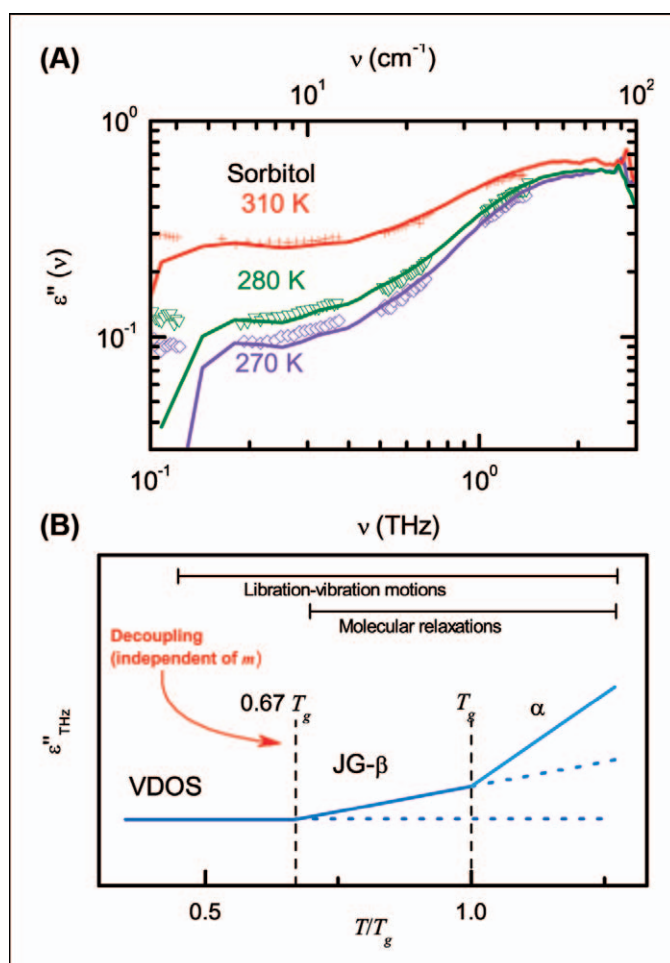


**Fig. 6.** (A) Comparison of dielectric losses at terahertz frequencies as obtained by dielectric spectroscopy (data points, from Kastner et al.<sup>110</sup>) and terahertz spectroscopy (solid lines, modified from Sibik et al.<sup>124</sup>) for sorbitol at 270–310 K. (B) Schematic of the thermal decoupling process of the molecular relaxation processes from the VDOS, or microscopic peak, in supercooled hydrogen-bonded liquids (modified from Sibik et al.<sup>124</sup>).

is true, it is reasonable to expect no contribution of the Boson peak to terahertz radiation.

With the advent of THz-TDS, it has become possible to directly access terahertz frequencies experimentally. In comparison to conventional dielectric spectroscopy, THz-TDS has some advantages, such as that it is a noncontact method and that measuring spectral data over a broad temperature range is straightforward. Sibik and coworkers showed that the absorption of sorbitol is close to zero at 0.7 THz at temperatures well below the glass transition temperature, which is in agreement with the work by Ruta et al. and further supports a non-optical origin of the Boson peak in the case of sorbitol glass.<sup>123,124</sup>

While a number of studies have been used to characterize inorganic glasses using THz-TDS<sup>125,126</sup> where it was possible to resolve the charge distribution

and to observe the Ioffe–Regel transition,<sup>127,128</sup> the properties of hydrogen-bonded glasses at terahertz frequencies have only recently attracted attention. Zeitler et al. demonstrated that in situ THz-TDS can be used to study both the relaxation and crystallization processes of small organic molecules in the amorphous state.<sup>129</sup> Following the same principle, McIntosh et al. investigated the water-vapor-induced crystallization of amorphous lactose,<sup>130</sup> and Sibik et al. investigated the spectral changes associated with the onset of crystallization in supercooled paracetamol.<sup>131</sup> Very few experimental studies have investigated the relaxation processes of polymers using THz-TDS. Thus far, only Wietzke et al. described the effects of the glass transition in weakly absorbing polymers and how the refractive index changes as the material turns from a rubber into a glass.<sup>132</sup> For the polyalcohols (glycerol, threitol, xylitol, and sorbitol) as well as sorbitol–water mixtures, Sibik and coworkers investigated the decoupling of the dielectric relaxation processes from the VDOS (Fig. 6B) as the sample materials were cooled from a supercooled liquid to a glass and further to temperatures well below  $T_g$ .<sup>123,124</sup>

Three universal features were observed in the dielectric losses (Fig. 6a): (1) at temperatures well below the glass transition, is a temperature-independent VDOS peak, which persists into the liquid phase and which has been identified as being due to librational–torsional modes. (2) For  $0.65 T_g < T < T_g$ , an additional thermally dependent JG  $\beta$  relaxation process was observed. Clear spectroscopic evidence was found for a  $\beta$  glass transition at  $0.65 T_g$ , which is not related to the fragility of the glasses and which appears to be a universal feature of hydrogen-bonded glasses. (3) At temperatures above  $T_g$ , the  $\alpha$  relaxation processes dominated the spectra. In addition, Sibik et al. highlighted that the thermal changes in the losses at terahertz frequencies originate from a universal change in the hydrogen-bonding structure of the samples.<sup>124</sup>

**Liquid Crystals.** At this point, it is interesting to note that recently several groups have considered the properties of liquid crystals (LCs) in the terahertz frequency range. Liquid crystals are a distinct phase of matter occurring between the (isotropic) liquid and crystalline states (of which there are various subphases, such as nematic, smectic, and cholesteric). In contrast to an isotropic state, which by definition has no long-range order, and the crystalline states, which have long-range periodic order in three dimensions, LCs are in the middle, containing some degree of alignment. This degree of alignment, combined with the anisotropy of the molecules (they are normally long and thin), leads to an anisotropy in the observed parameters, including birefringence and dielectric anisotropy. These properties have led to researchers finding LCs enormously useful in display technologies in the past half century because the refractive index can be precisely controlled using electric or magnetic fields, allowing the light

propagation to be manipulated.<sup>133</sup> As terahertz technologies have become more mature, groups have begun to investigate the properties of LCs in this low-frequency region to evaluate whether they may be as useful in developing terahertz-frequency optical devices.

Early measurements of the terahertz properties of LCs were on pure materials such as 4-(*trans*-4'-pentylcyclohexyl)-benzonitrile (PCH-5),<sup>134</sup> and 4-cyano-4'-n-pentylbiphenyl (5-CB), 4-cyano-4'-n-hexylbiphenyl (6-CB), 4-cyano-4'-n-heptylbiphenyl (7-CB), and 4-cyano-4'-n-octylbiphenyl (8-CB).<sup>135–138</sup> While the terahertz birefringence for PCH-5 was found to be much smaller than at optical frequencies, the cyano-biphenyl (CB) family of LCs were generally observed to display birefringences at terahertz frequencies that were similar to (or slightly smaller than) optical frequencies, and as the temperature approaches the clearing temperature (i.e., the LC–isotropic transition), the ordinary and extraordinary refractive indices were observed to converge to a single value, normally closer to the ordinary refractive index than the extraordinary. In general, the absorption was found to be relatively low, on the order of  $10 \text{ cm}^{-1}$ , and increasing with frequency, with the ordinary absorption coefficient being higher than the extraordinary absorption coefficient.<sup>137,138</sup> This increase and anisotropy in absorption coefficient were attributed in these LCs to torsional motions of the phenyl rings along the short molecular axis, often called Poley absorptions.<sup>139</sup>

Despite the usefulness of probing pure materials, many LCs are actually mixtures, the compositions of which are kept secret. As a result, much recent research has been done on these mixtures, including E-7, BL-037, RDP-94990, RDP-97304, and negative dielectric anisotropy materials MLC-7029 and MLC-1808.<sup>140–143</sup> In particular, efforts have been made to find high-birefringent materials because, otherwise, very thick LC cells are required, which result in switching times in the hundreds of seconds. At the same time, absorption can become significant at the potentially millimeter thicknesses required for terahertz optical devices, making the choice of LC mixture an important consideration.

Ultrabroadband spectroscopy is a key advancement in the area of understanding the terahertz optical properties of LCs because it allows the rotational and other intramolecular vibrations that appear in the high-terahertz-frequency region, the tails of which dominate the more commonly accessed low-terahertz-frequency region, to be observed and characterized. Vieweg et al. studied 5-CB using an ultrabroadband terahertz spectrometer and performed computational calculations on the molecule.<sup>144</sup> They demonstrated that, above 4 THz, the spectrum is dominated by strong intramolecular vibrational modes, particularly in the ordinary orientation. They observed significant discrepancies in their calculations below 3 THz, however, and attributed this to disorder-induced coupling between the electromagnetic field and the VDOS, similar to the Ioffe–Regel transition observed in inorganic glasses.<sup>128</sup>



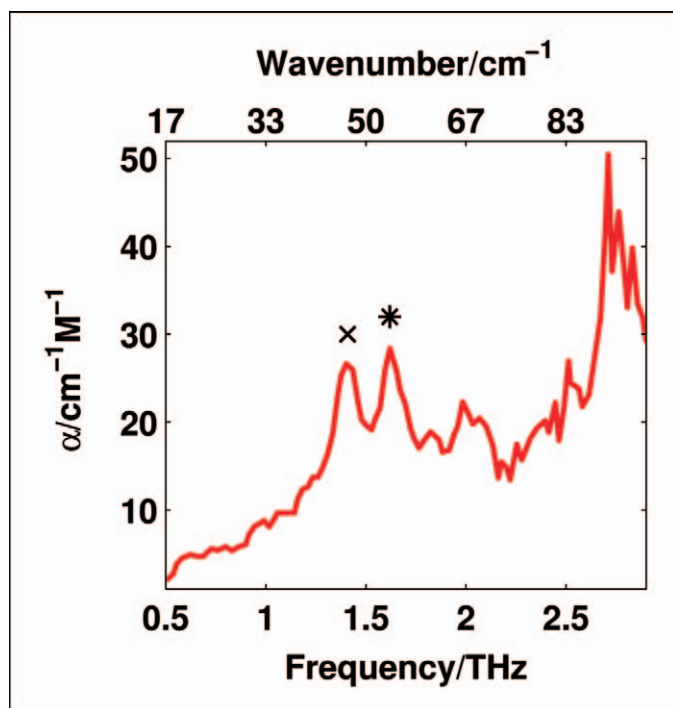


Fig. 7. Terahertz spectra of all-trans retinal (adapted from Walther et al.<sup>145</sup>).

## CRYSTALLINE SYSTEMS

In contrast to the monotonically increasing and relatively featureless spectra that are observed at terahertz frequencies for liquids and amorphous materials, in crystalline solids distinct spectral features can be measured using terahertz or low-frequency Raman spectroscopy. Compared to the vibrational modes that are observed at higher frequencies in the IR and NIR, the nature of the fundamental modes that are observed below 10 THz are more complex in that they are often strongly influenced by coupling between intramolecular and intermolecular modes, albeit for the most rigid molecules, and are much more sensitive to intermolecular interactions, particularly for hydrogen-bonded molecular crystals given that the hydrogen-bonding energy falls directly into the photon energy of terahertz frequencies.

**Probing Static Systems.** The early work on crystalline systems using THz-TDS focused on biomolecular systems such as isomers of retinal, where the use of the different molecular structures allowed researchers to propose tentative assignments to the features observed in the terahertz spectra. Walther et al. concluded that the feature that occurs at  $54\text{ cm}^{-1}$  (highlighted with a star in Fig. 7) in all three isomers is localized to the phenyl ring, whereas the  $47\text{ cm}^{-1}$  feature that was strongest in the all-trans isomer (highlighted with a cross in Fig. 7) is localized in the terminal part of the chain.<sup>145</sup> Later work from Walther and coworkers considered a series of

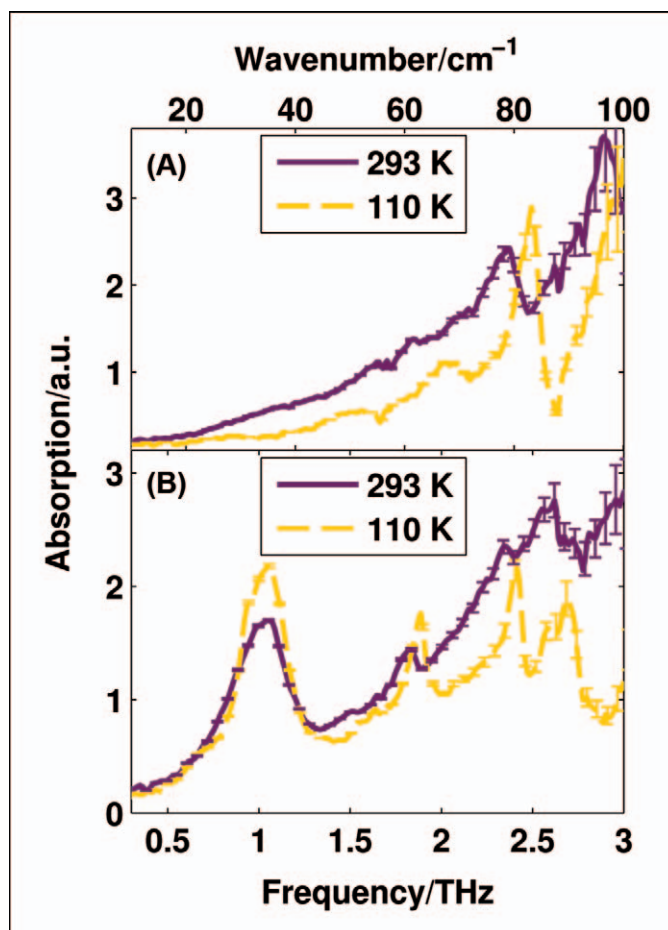


Fig. 8. Terahertz spectra. (A) DL-Tartaric acid measured at 293 K (purple solid line) and 110 K (gold dashed line). (B) L-Tartaric acid measured at 293 K (purple solid line) and 110 K (gold dashed line). Clear differences are observed between the two spectra, particularly at lower temperatures at which the various vibrational modes are further resolved.

different conformers of saccharides, and in this case, they concluded that the observed spectral features were due to noncovalent, intermolecular bond vibrations.<sup>146</sup> In fact, intermolecular interactions play an important role in the observed terahertz spectra of many crystalline materials. For example, the terahertz spectra of crystalline chiral and racemic forms of tartaric acid are shown in Fig. 8. Despite the identical chemical composition, the terahertz spectra are very different due to the differences in the crystal structure that arise as a result of the different chiral forms used. This sensitivity to intermolecular arrangement arises from the energies and length scales that the terahertz frequency range probes, and because the crystal structure has an effect on the physical properties of a material, this information is of interest, particularly in the area of pharmaceutical research.

The identification of polymorphs, in particular, has been extensively studied using THz-TDS. Polymorphs,

## focal point review

different supramolecular crystalline structures of the same molecule, are of interest in the pharmaceutical industry because of the changes these polymorphs can give to the physical properties of the materials, including melting points and solvation ability. However, because the different polymorphs are chemically identical, high-frequency techniques such as mid-IR and conventional Raman spectroscopy reveal only subtle differences, whereas the low-frequency techniques, such as THz-TDS, probe the differences in the intermolecular bonds that result from these different crystalline structures. Some of the earliest work in this area by Strachan and coworkers showed that the crystalline species of carbamazepine (CBZ), enalapril malaete, indomethacin, and fenopropen calcium were all different due to their differing lattice vibrational modes. Furthermore, the crystallinity and loadings of these different materials could be quantified using a partial least squares technique.<sup>147,148</sup> At about the same time, work by Upadhyaya et al. focused on different forms of saccharides and found that the unit cell structure and precise chemical composition of the saccharide altered the terahertz spectra.<sup>149,150</sup> Soon after, quantitative measurements of amino acid concentrations in mixtures were demonstrated, and researchers were able to identify with high reproducibility which amino acids were present and in what proportions.<sup>151</sup>

Polymorphic screening, in particular, has become a popular test using low-frequency Raman spectroscopy. Prior to this relatively recent surge in low-frequency Raman spectroscopy there were a number of studies of the spectral properties of hydrogen-bonding systems, as reviewed by Colaianne and Nielsen.<sup>152</sup> Raman-active bands below  $200\text{ cm}^{-1}$  were shown to provide reliable information for characterizing the solid forms of oxcarbazepine and chlorpropamide, and following the temperature-induced phase transformation of olanzapine,<sup>153</sup> although the isolated molecule calculations used struggled to reproduce the experimental results below  $70\text{ cm}^{-1}$ . Organic semiconductors such as  $\alpha$ -quaterthiophene have also been shown to contain Raman-active phonon modes, and the low- and high-temperature polymorphs were characterized, giving insights into the relative stabilities of the two structures.<sup>154</sup> Chemometric analysis of mixtures, such as the work by Lamshöft et al. studying  $n$ -component mixtures of sulfonamides,<sup>155</sup> have demonstrated that techniques commonly used in the mid-IR region are also applicable to this frequency region. The majority of recent studies, however, have focused on semi-qualitative chemical fingerprinting, with demonstrations of active pharmaceutical ingredient (API) specificity, including chemicals such as CBZ;<sup>156–158</sup> ibuprofen, aspirin, and paracetamol (acetaminophen);<sup>159</sup> caffeine, theophylline, and apixaban;<sup>158</sup> paracetamol, flufenamic acid, and imipramine hydrochloride;<sup>160</sup> and respirable powders.<sup>161</sup> For CBZ, the Raman intensity increases markedly below  $200\text{ cm}^{-1}$ , which has been tentatively attributed to the large change in polarizability for these

vibrations, derived from changes in the  $\sigma$ - $\pi$  back-bonding between the amide and aryl groups.<sup>158</sup> This observation appears to hold true for many of the other APIs investigated as well, in which an approximately fivefold increase in Raman intensity is seen when comparing the low-frequency region ( $10$ – $400\text{ cm}^{-1}$ ) and the fingerprint region ( $400$ – $1600\text{ cm}^{-1}$ ).<sup>160</sup> Whether this is a result of large changes in polarizabilities due to the presence of  $\pi$ -bonding rich moieties in many APIs or a more fundamental characteristic of low-frequency Raman is unclear at this stage.

Aside from probing the structural effects resulting from different chemical forms, Yamaguchi et al. used THz-TDS to investigate the effects of the enantiometric form of materials on the terahertz spectra for alanine.<sup>162</sup> Although the D- and L- (i.e., chiral) forms were found to be very similar, with reported absorption bands at  $74.4$  and  $85.7\text{ cm}^{-1}$ , only a single band at  $41.8\text{ cm}^{-1}$  was observed for the DL- (i.e., racemic) forms. What is significant, however, is that, even though both the chiral and racemic structures are similar to each other in both cell dimensions and predicted structures, their terahertz spectra differ greatly in agreement with previous studies based on low-frequency Raman spectroscopy.<sup>163</sup> To test this sensitivity at the logical limit, Parrott et al. studied two cocrystal systems containing structurally and chemically identical cocrystals that exhibited different physical properties (e.g., melting points).<sup>164</sup> The difference between them was the enantiometric composition of one of the cocrystal formers; in one case the chiral form was used, whereas in the other case the racemic form was used. The cocrystals, formed of theophylline (Tp) and either the L- or DL- form of malic acid, had very similar X-ray powder diffraction (XRPD) patterns due to their essentially identical unit cells (see Fig. 9A), yet the terahertz spectra of the two cocrystals were very different, particularly at low temperatures (Fig. 9B). Computational studies suggested that one of the two malic acids in the chiral cocrystal is strained, leading to a broken symmetry in the energy of the system. Consequently, there are many more vibrational modes for the chiral cocrystal than for the racemic cocrystal, despite their similarity in structure.

Further examples that both demonstrate the high sensitivity of THz-TDS for supermolecular structure and explain this sensitivity at the molecular level by means of computational techniques (as discussed in more detail in the next section) are the recent studies by Delaney and coworkers on the conformational disorder in irbesartan<sup>165</sup> and on the interplay between conformational strain and cohesion binding that was found to play a key role in the stability of gabapentin polymorphs<sup>166</sup> as well as aripiprazole,<sup>167</sup> and by Pellizzeri et al. on how THz-TDS can play an important role as a complementary technique to X-ray diffraction in the characterization of new polymorphs.<sup>168</sup> Succinonitrile forms a plastic crystal that is flexible and exhibits strong disorder in its crystalline phase at room temperature but that can be

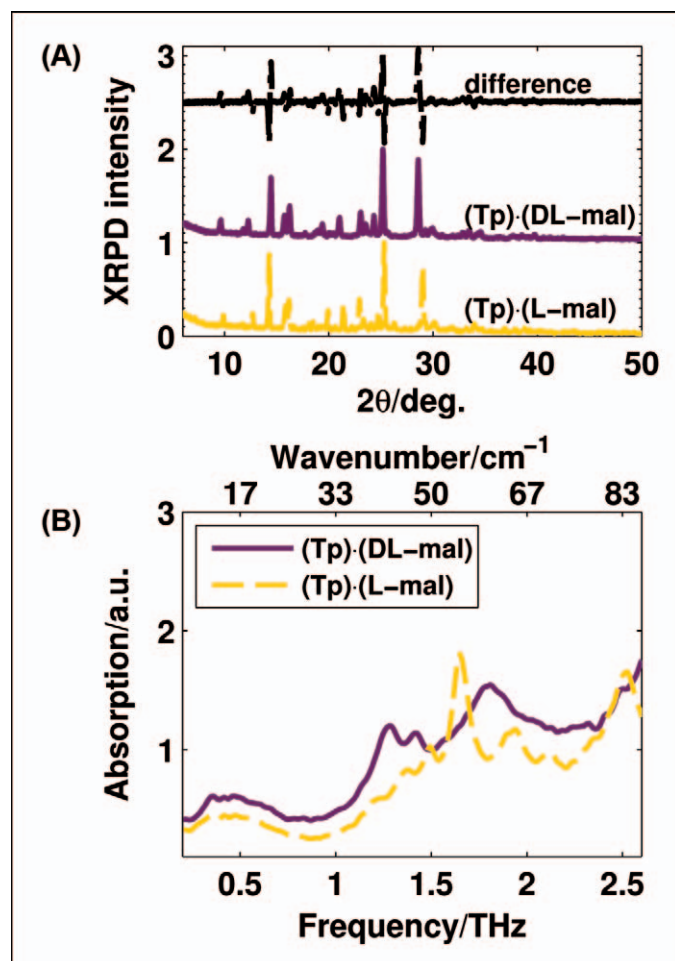


Fig. 9. (A) The XRPD patterns for (Tp)•(L-malic) (bottom, gold dashed line) and (Tp)•(DL-malic) (middle, purple solid line), and the difference between them (top, black dashed line). (B) Terahertz spectra at 110 K (data from Parrott et al.<sup>164</sup>).

“frozen out” at lower temperature, leading to a much more ordered, rigid-crystal phase that exhibits distinct, albeit broad, spectra features at terahertz frequencies.<sup>169</sup> This study made a nice connection among the spectra originating from well-defined crystal structures; slightly disordered systems such as benzoic acid, where symmetry breaking is observed;<sup>170</sup> and the even more disordered LCs discussed earlier.<sup>144</sup> The data indicate that the terahertz vibrational modes broaden with increasing disorder in the intermolecular interaction compared at the same temperature (i.e., independent of the effect of  $kT$  compared to  $h\nu$ ). Crystalline disorder forms a continuum from well-defined relatively narrow peaks that are detected for the most-ordered structures such as single crystals<sup>171</sup> or thin films<sup>172–177</sup> all the way to the complete breakdown of the vibrational modes into the VDOS (as discussed in the section on Mesoscopic Structure and Dynamics for amorphous samples) or as a result of polymerization.<sup>178</sup> For example, using crystalline and amorphous poly(3-hydroxybutyrate), Hoshina

and colleagues<sup>179–182</sup> and Yamamoto et al.<sup>183</sup> studied this effect on a polymer system by combining far-IR spectra, low-frequency Raman spectra, and computational methods.

Although THz-TDS makes it possible to probe the structural and energetic changes in the crystalline lattice, it is generally not possible to elucidate information on the actual structure of the system directly from the terahertz spectra; unlike in the mid-IR, particular frequencies do not correspond to specific structural motifs. In general, powdered samples pressed into pellets are used to measure the terahertz spectral properties of a given crystalline compound. In these cases, the crystals are assumed to have a random orientation, and so the vibrational eigenvectors are assumed to be integrated equally along all orientations. However, because the terahertz radiation from emitters is generally polarized in one orientation,<sup>184,185</sup> it is possible to measure the orientation dependence of the terahertz modes if a single crystal of the material can be grown large enough. Rungsawang et al. demonstrated this using single crystals of L-cysteine and L-histidine, and they observed large differences in the spectra as the single crystals were rotated.<sup>186</sup> A similar approach, together with computational methods, was used by Singh et al. to better understand the nature of the vibrational modes that can be observed at terahertz frequencies.<sup>187</sup> In addition, by spatially separating molecules in mesoporous silicates and comparing the spectra acquired from the spatially separated molecules with the measurements from the polycrystalline sample powder, Ueno et al.<sup>188</sup> and Ueno and Ajito<sup>189</sup> showed experimentally that some of the modes observed in the terahertz spectra clearly are intermolecular.

**Probing Reaction Dynamics.** Given the sensitivity of terahertz spectroscopy to both structural and energetic changes, the obvious extension to its use in crystalline systems was to study solid-state transformation processes. In principle, terahertz spectroscopy can be employed to follow any solid-state transformation, with time resolution being the single largest practical limiting factor (currently tens of seconds). As rapid-scanning systems improve, this will become less of an issue. Studies to date have mostly focused on reversible reactions that can have their reaction rates limited and controlled through external parameters such as temperature and humidity. Liu and Zhang<sup>190</sup> demonstrated the ability to use THz-TDS to follow the dehydration reaction of D-glucose monohydrate at various temperatures. By monitoring the growth of an anhydrate feature at 1.4 THz, it was possible to probe the kinetics of the particular reaction. In this case, the two-dimensional phase-boundary-controlled reaction was found to be the model that most closely resembled the observed kinetics (see Fig. 10), representing the egress of water from the crystalline system. Zeitler and coworkers probed the phase transformation of CBZ using THz-TDS.<sup>191,192</sup> The transformation of CBZ from form III to form I was



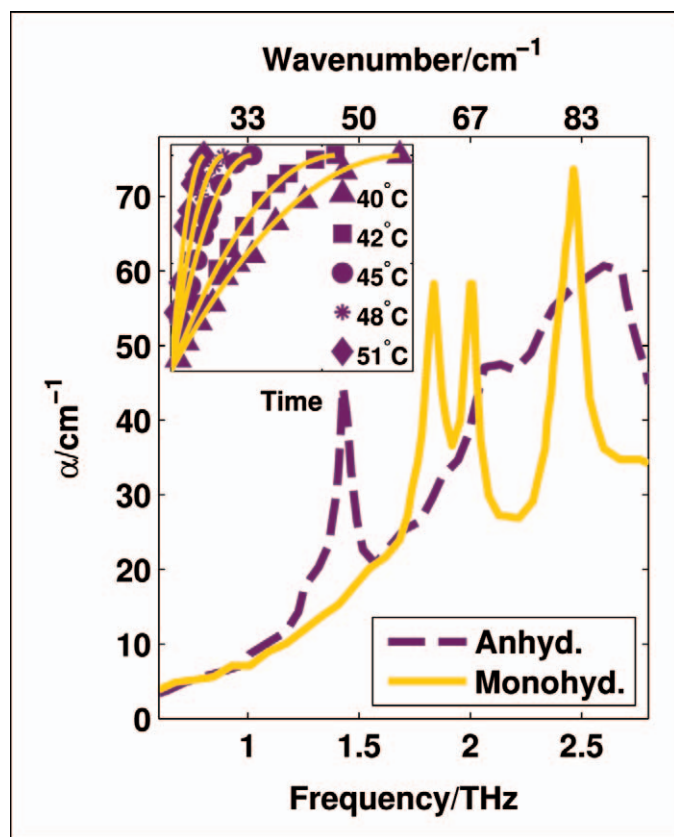


Fig. 10. Terahertz spectra of the anhydrate (purple solid line) and monohydrate (gold dashed line) forms of *D*-glucose. Inset: the resulting kinetic model fits at different temperatures. (Adapted from Liu and Zhang.<sup>190</sup>)

observed at 433 K, and the growth and decay of the two forms were followed by observing the change in the terahertz spectra (Fig. 11A); in particular, a simple principal component analysis (PCA) was used to measure the percentages of form III and form I at any point during the reaction. They observed that the fractions of form III and form I did not change at the same rate, evidence that the reaction involved a sublimation phase (see Fig. 11B).

The same group also investigated the complex polymorphism of sulfathiazole and the solid-state phase transitions between the different forms. Polymorphs I and II were easily distinguished from forms III–V using mid-IR spectroscopy; however, it was not possible to differentiate among forms III, IV, and V using FT-IR spectroscopy. In contrast, X-ray diffraction techniques should distinguish the different forms in principle but, due to preferred orientation effects, this was almost impossible in practice, as outlined by Threlfall.<sup>193</sup> It was possible to easily distinguish among all five polymorphs that were studied using both THz-TDS and low-frequency Raman spectroscopy.<sup>194</sup>

Low-frequency Raman spectroscopy has been used to investigate solid-state transformations, usually as part of

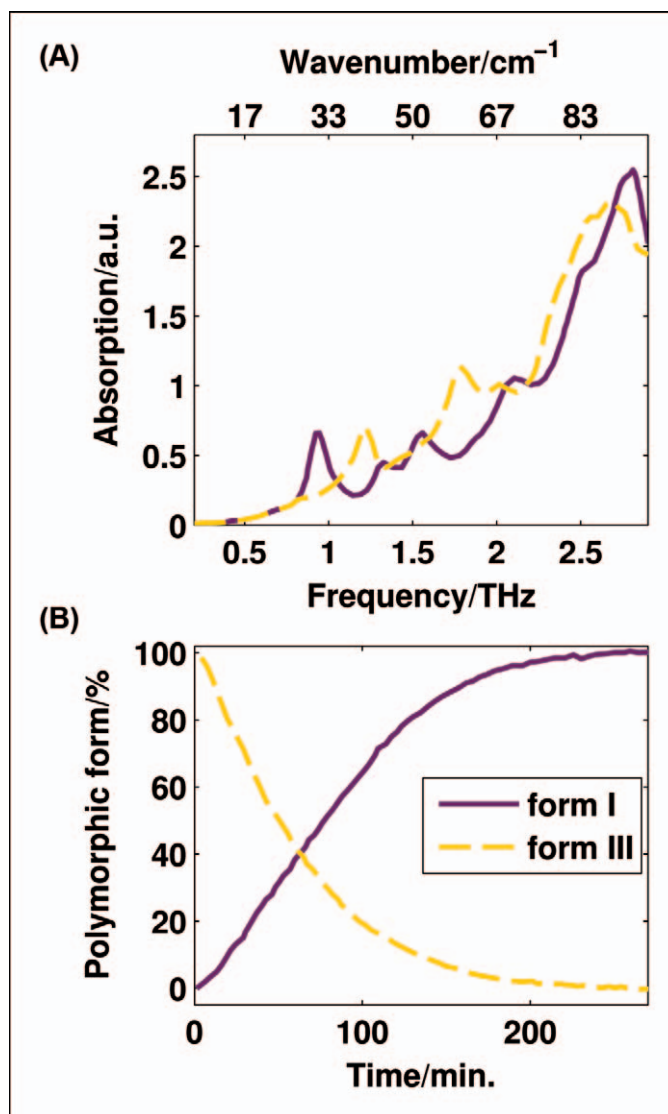


Fig. 11. (A) Terahertz spectra of form I (purple solid line) and form III (gold dashed line) CBZ. (B) Percentage of the polymorphic form in the solid state, derived from the PCA analysis of the terahertz spectra. (Adapted from Zeitler et al.<sup>192</sup>)

a crystallization from an amorphous form. The crystallization of indomethacin, paracetamol (acetaminophen), and caffeine from their amorphous states have been probed using low-frequency Raman spectroscopy.<sup>195–197</sup> In the case of indomethacin, low-frequency Raman measurements indicated that amorphous indomethacin prepared via cryogrinding partially crystallized to the  $\gamma$  form at room temperature, well below the glass transition temperature of 43 °C, and that the peak evolution fitted a site-saturation and two-dimensional growth mechanism.<sup>195</sup> Furthermore, pressure-dependent low-frequency Raman measurements of the  $\gamma$  form showed that the phonon peaks in this region shifted to a higher frequency with pressure, confirming the higher-frequency results

suggesting that the crystal was moving into a denser phase. Furthermore, continued grinding broadened the phonon modes, suggesting a disruption of the dimer chains and the onset of amorphization.<sup>197</sup> Most recently, the polymorphic transformations of caffeine from the amorphous state were studied in more detail.<sup>198</sup> Caffeine exists in two crystalline versions: form I and form II. Using low-frequency Raman spectroscopy, form I was observed to transform into another metastable state on moderate pressurization. This was the first time such a state had been observed, due to the rapid-acquisition characteristics of Raman spectroscopy. Further pressurization results in a disordered state, suggesting pressure-induced amorphization.

Sibik et al. showed using paracetamol that THz-TDS can be used to investigate the crystallization and subsequent phase transformations, starting with the supercooled phase of paracetamol.<sup>131</sup> Due to the high sensitivity of THz-TDS to intermolecular interactions, it was possible to determine the onset of crystallization very precisely and quantify the crystallization kinetics. Following the crystallization into form III, further phase transitions to forms II and I were observed before the sample melted. Using the slightly higher band width on a far-IR spectrometer, Suzuki et al. showed using cyclohexanol that the phonon spectra can be used to determine the kinetics of complex isothermal phase transitions at temperatures up to 230 K.<sup>199</sup> At higher temperatures, the SNR that can be achieved using bolometric detection was likely to decrease and the TDS method was more suitable, although the spectral band width would be significantly smaller. Rather than inducing crystallization through heating, McIntosh et al. exposed amorphous lactose to a high relative humidity and monitored the crystallization process using THz-TDS.<sup>130</sup>

Apart from following solid-state transformations, it is possible to follow solid-state reactions if there are observable absorption features in either the initial or final products. Furthermore, it is possible to observe intermediate states and therefore to elucidate some understanding of the reaction mechanism itself. Ge et al. monitored the crystal transformation of a mixture of *p*-benzoquinone and *p*-dihydroxybenzene to quinhydrone, although the quantitative analysis was complicated by the multiple overlapping features of the reagents and products, no doubt due to the similar structures of the reagents.<sup>200</sup> Quantitative analysis was possible for the co-crystallization reaction of phenazine and mezaconic acid, which were specifically chosen by Nguyen et al. because the reagents were relatively featureless around 1.2 THz, where a large co-crystal product peak is located.<sup>201</sup> By following the evolution of this peak, the researchers surmised that the mechanical action of grinding resulted in an amorphous phase that recrystallized upon standing for a number of days to the pure crystalline cocystal product. Liu et al. monitored the reaction between L-tartaric acid and sodium carbonate

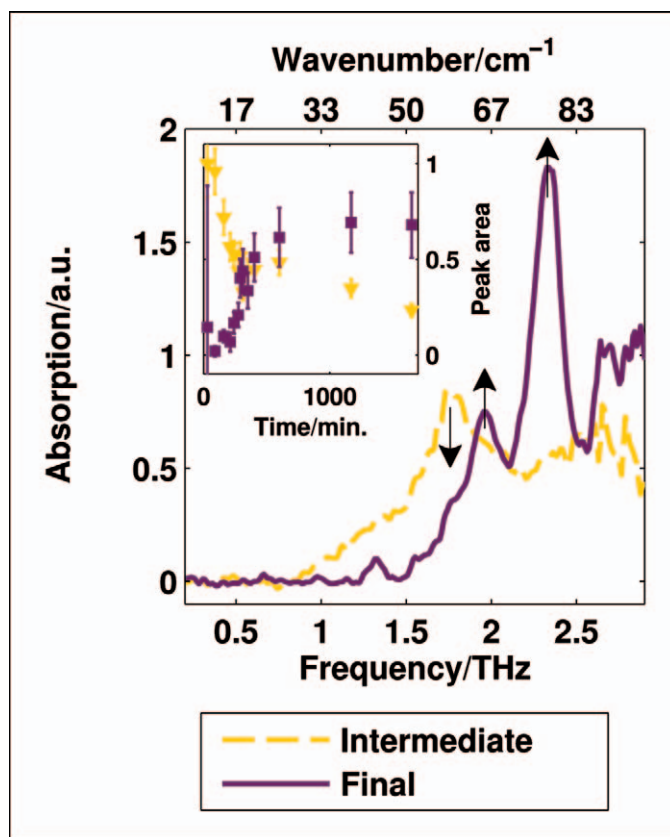


**Fig. 12.** Terahertz spectra of the intermediate (gold dashed line) and final cocystal (purple solid line) of the theobromine-oxalic acid cocystal, with the growth/decay of features highlighted using arrows. Inset: Evolution of the peak areas with times for the features centered at 1.75 THz (gold triangles) and 2.34 THz (purple squares).

monohydrate by following the decrease in the L-tartaric acid feature at 1.08 THz; in contrast, the product was relatively featureless.<sup>202</sup> By considering a number of kinetics models, the authors concluded that the reaction followed a three-dimensional diffusion mechanism. Recently, the present authors considered the solid-state, mechanically activated reaction between theobromine and oxalic acid that had been observed to be moisture sensitive. A clear intermediate state (see Fig. 12) is observed to transition to the final state during approximately 400 min of standing in a humid environment post-grinding. Through the use of kinetics models, the authors proposed a moisture-mediated reaction mechanism for this reaction. These measurements represent initial exploratory tests of the potential of terahertz spectroscopy; in situ reaction monitoring may provide a useful application of the technology in the future.

**Beyond Phase Transformations.** The specific frequency range of terahertz radiation means that it is accessing low-energy inter- and intramolecular vibrations. The information contained in this range can have a bearing on the specific physical properties of the

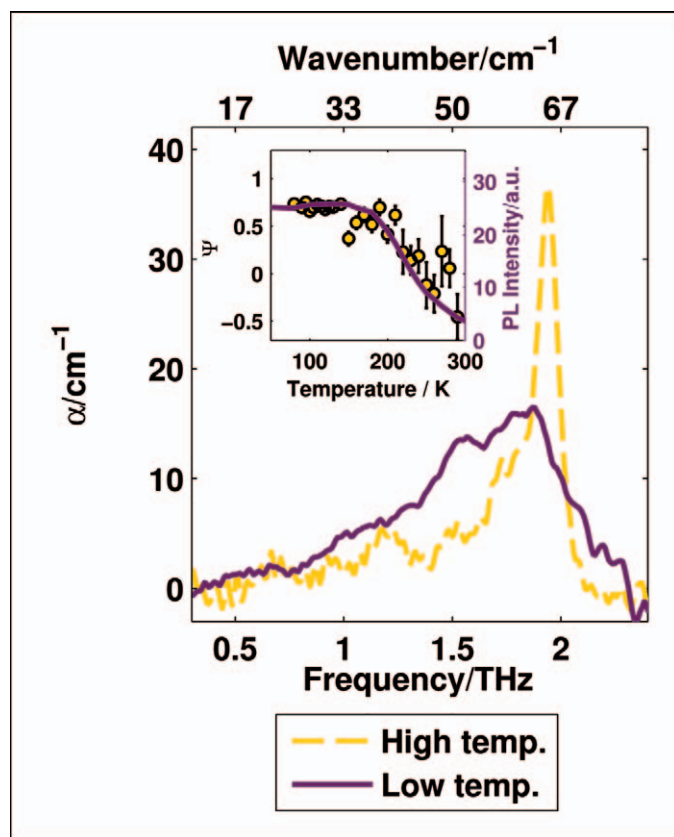


**Fig. 13.** Terahertz spectra of TPE measured at low (gold dashed line) and high (purple solid line) temperatures. Inset: Comparison of the trends of PL intensity and peak ratio  $\Psi$  as a function of temperature, highlighting the correlation. (Adapted from Parrott et al.<sup>203</sup>)

materials. One example of such a situation is fluorescence. A fluorescent material generally absorbs light energy of a particular wavelength and then emits this energy at a different frequency. However, competing with this radiative energy transfer are other energy-loss mechanisms, which can include low-frequency rotations of the molecule. One such family of materials that exhibit this trait are known as aggregation-induced emission (AIE) molecules, which increase the strength of the fluorescence intensity upon aggregation. To understand the underlying mechanism for this, Parrott et al. measured the fluorescence (also known as photoluminescence [PL]) intensity of tetraphenylethylene (TPE) with temperature in the solid state.<sup>203</sup> We found that the terahertz spectra changed remarkably between low and high temperatures (see Fig. 13), although no phase transformation was observed using other techniques. X-ray diffraction studies suggested a small change in the unit cell occurred between low and high temperatures, but with no further information between the two extremes, little could be gleaned from these data. However, by comparing the relative strengths of absorption features in two areas of the terahertz spectrum, the

authors were able to observe a remarkable correlation between this relative strength and the PL intensity. Computational studies linked these vibrations to intramolecular vibrations, thereby helping to explain the mechanism of AIE. In particular, this result highlights the growing importance of using computational techniques to interpret the observed terahertz spectra; therefore, it is not surprising that in recent years many publications in the area of crystalline terahertz spectroscopy have focused on the computational techniques used to understand them.

## COMPUTATIONAL TECHNIQUES

The computational techniques employed in terahertz and low-frequency Raman spectroscopy are used to calculate the vibrational modes of a solid and have grown out of a branch of computational chemistry that stems from the initial release of Gaussian in the 1970s. In the mid-IR region, the Gaussian computer program uses ab initio methods to estimate the vibrational frequencies of a molecule and the corresponding IR and Raman intensities. Because the computational power required scales to the power of the number of atoms, this technique uses a single-molecule representation (i.e., the gas phase) to limit the time it takes to perform the calculation. At IR frequencies, this has little effect on the accuracy of the calculated modes in the solid state because the vibrational modes are limited to high-frequency intramolecular bond stretches, such as the broad O–H bond stretch found around 3000  $\text{cm}^{-1}$ . Initially, computational investigations accompanying terahertz spectroscopic measurements were confined to single-molecule treatments, such as Chen et al. on 2-4-dinitrotoluene,<sup>204</sup> Ning et al., on methamphetamine,<sup>205</sup> and Rungsawang et al. on amino acid single-crystal measurements.<sup>186</sup> However, even these early studies highlighted the inherent weakness of single-molecule calculations when considering a solid crystalline state—the lack of treatment of intermolecular interactions. For example, using the THz-TDS spectra of cysteine three modes were observed between 40 and 93  $\text{cm}^{-1}$ , yet Gaussian predicted only a single feature.<sup>186</sup> As Tomerini and Day explained in their recent article,<sup>206</sup> the use of single modes to explain the origin of features in the terahertz spectrum can be dangerous. A classic example is the analysis of the low-frequency modes of 3,4-methylenedioxyamphetamine (MDMA, or ecstasy) performed by Allis et al.<sup>207</sup> and Hakey et al.,<sup>208</sup> in which three modes at 37.0, 59.3, and 86.6  $\text{cm}^{-1}$  were identified from the experimental spectrum. Isolated-molecule calculations yielded very similar modes, attributed to internal torsional, bending, and rocking modes, which might be erroneously attributed to the observed spectrum. A crystal calculation found similar mode frequencies, but the origins were very different: the two lowest modes were assigned to rigid molecule rotations and translations, intermolecular vibrations. The intramolecular vibrations observed in the single-mole-



cule calculations were found to shift out of this frequency range due to coupling with the crystal environment. Consequently, due to the low energy of the terahertz region and the propensity for intermolecular interactions to dominate the vibrational response, either as a direct motion or through coupling to intramolecular modes, researchers should resist the convenience of using single-molecule calculations to interpret terahertz-region spectra.

Therefore, to correctly calculate the terahertz spectrum for a crystalline material, methods that consider the molecular arrangement of the periodic structure and the associated intermolecular interactions of the crystal must be used. The technique that has received considerable interest in recent years involves quantum mechanical electronic structure calculations because all the relevant forces must ultimately arise from the electrostatic interactions between the electrons and nuclei of the system. Density functional theory (DFT) is most commonly applied to perform this type of calculation, and a number of techniques and programs exist that differ in how they define the basis sets defining the electronic density. These may either be localized basis sets (such as the atomic-like orbitals used in DMol<sup>209</sup> and SIESTA,<sup>210</sup> and the Gaussian wavefunctions used in the CRYSTAL<sup>211</sup> package) or plane-wave basis sets (such as those implemented in CASTEP<sup>212</sup> and VASP<sup>213</sup>). Examples using all three types of functions have been published in the terahertz literature, but the most commonly used codes nowadays are CRYSTAL and CASTEP.

Allis et al.<sup>207,214</sup> and Allis and Korter<sup>215</sup> published a large body of research developing the use of numerical techniques to calculate vibrational frequencies of crystalline materials in the terahertz region. High-explosive materials, such as HMX,<sup>214</sup> PETN,<sup>215</sup> and RDX,<sup>207</sup> were used as test beds of the importance of using intermolecular interaction (i.e., solid-state) calculations instead of isolated molecule calculations. For HMX and PETN, Gaussian03 (isolated molecule) and DMol3 (isolated molecule and solid-state) calculations were compared to experimental spectra of the explosives, and in both cases, the isolated-molecule calculations were seen to be incapable of reproducing the observed spectral features; solid-state calculations were required. Nevertheless, despite its relative speed (through the use of atomic-like orbitals), DMol3 has a drawback in that it is unable to effectively calculate the vibrational intensities. Consequently, later research by King et al.,<sup>216</sup> Hakey and coworkers,<sup>217,218</sup> and King and Korter<sup>219</sup> has focused on the use of CRYSTAL, with which they have successfully predicted the vibrational frequencies and intensities at terahertz frequencies for L- and DL-serine,<sup>216</sup> methamphetamine hydrochloride,<sup>217</sup> ketamine hydrochloride,<sup>218</sup> and the anhydrous and dihydrate forms of oxalic acid.<sup>219</sup> A major component of these studies is the determination of the best density functional to use in the calculations. The density functional is used to describe the electron density of the system, and many (rather elaborate) forms

have been developed, which include a dependence on the gradient of the electron density (generalized gradient approximation) and can also include the exact exchange energy as calculated from Hartree–Fock wavefunctions (known as hybrid functionals). Nevertheless, there appears to be no hard and fast rule for determining a “best” functional for terahertz spectral calculations because the different approximations used in each functional can be more or less important for a particular structure; consequently, a poor choice of DFT functional can have a large effect on the quality of the simulated spectrum.

Benzoic acid has been the molecule of choice for comparisons of experimental terahertz spectra with theoretical predictions from the CASTEP code,<sup>170,220–222</sup> no doubt due to its well-formed intermolecular hydrogen-bonding interactions. The CASTEP simulations have reproduced the correct number of modes, mode strength, and approximate positions, but they often (as in these cases) slightly overestimate the vibrational frequencies (due to the lack of treatment of anharmonicity). Moreover, the benzoic acid dimer structure is actually an interesting problem because two possible forms for the hydrogen-bond dimer configurations exist. The mixing of these forms is not necessarily ordered, and so it poses a difficulty for DFT methods because the easiest way of accounting for it is to increase the supercell, which increases the computational time exponentially. In this case, rigid-molecule approximations, such as DMAREL, can produce a computationally cheap approximation to the intermolecular modes.<sup>170,223–225</sup> Such an approach can be successful only if the molecules themselves are very rigid because flexible molecules often result in significant mixing of inter- and intramolecular modes.

Most recently, computational studies have focused on calculating the degree of mode mixing, accounting for particle shape and morphology, and incorporating dispersion corrections.

**Mode-Mixing and Morphology Effects Studies.** The quantum mechanical calculations that predict the vibrational frequencies and intensities also produce the displacement vectors for each motion. Using a technique first employed by Jepsen and Clark<sup>220</sup> and expanded on by later authors,<sup>226,227</sup> we can break down these displacement vectors into an intramolecular contribution and an intermolecular translation and libration contribution.

The total root mean square (rms), mass-weighted atomic displacement ( $d_{\text{total,rms}}$ ) for each molecule (of mass  $m_i$ ) for the particular vibrational mode is calculated as:

$$d_{\text{total,rms}} = \sqrt{\frac{1}{N} \sum_{i=1}^N m_i \delta_i^2} \quad (7)$$

where  $\delta_i$  is the displacement vector for the  $i$ th atom, obtained from the difference between the distorted atom position  $r_{1,i}$  and the equilibrium position  $r_{0,i}$ .

## focal point review

The contribution of translational motion of the molecule ( $d_{\text{trans,rms}}$ ) is therefore:

$$d_{\text{trans,rms}} = d_{\text{total,rms}} - \sqrt{\frac{1}{N} \sum_{i=1}^N m_i (r_{0,\text{CoM},i} - r_{1,\text{CoM},i})^2} \quad (8)$$

where  $r_{0,\text{CoM},i}$  and  $r_{1,\text{CoM},i}$  are the positions of each atom relative to the molecular center of mass. Next, the intramolecular contributions can be calculated by considering the rms difference between the equilibrium structure and the distorted structure:

$$d_{\text{intra,rms}} = \sqrt{\frac{1}{N} \sum_{i=1}^N m_i (r_{0,\text{CoM},i} - \mathbf{U}_{\text{min}} r_{1,\text{CoM},i})^2} \quad (9)$$

where  $\mathbf{U}_{\text{min}}$  is the optimized rotation matrix for the distorted configuration  $r_{1,\text{CoM},i}$ . As a result, the intramolecular contributions (Eq. 9) are known, and also the intermolecular ( $d_{\text{inter,rms}} = d_{\text{total,rms}} - d_{\text{intra,rms}}$ ) and rotational ( $d_{\text{rot,rms}} = d_{\text{inter,rms}} - d_{\text{trans,rms}}$ ) contributions can be determined.

An example of the characterization that can be achieved using these techniques is shown in Fig. 14, which clearly shows that while the higher-frequency modes are dominated by the internal vibrations of the molecule, the lower-frequency modes (4–9) are dominated by intermolecular translation and rotation.<sup>228</sup> A similar result was observed by Williams et. al.<sup>227</sup> in their computational study (using SIESTA) of the L- and DL-forms of valine, which show an increase in the intramolecular character of the vibrational mode beyond approximately 2.5 THz. Their extended follow-up study of DL-valine and DL-leucine again noted this increase, as well as expanding on ways of visualizing the vibrational character through use of a characterization strip to further analyze the relative intramolecular contributions to the motion from each functional group in the molecule. Most recently, Zhang et. al. performed a similar characterization on the calculated modes of adenine and adenosine using CRYSTAL09.<sup>229</sup> Although the adenine dimer had a clear distinction between the relative contributions of the translational-rotational intermolecular motions and the intramolecular vibrations (mode 46/ $\sim 175 \text{ cm}^{-1}$ ), the adenosine crystal structure had relatively high contributions from the intramolecular vibrations across the frequency range, no doubt due to the high flexibility of the adenosine molecule. Such a result shows that some systems can have mainly intermolecular nature at low frequencies but that this is system-dependent. In cases such as the adenosine system, rigid-molecule calculations would be unsuitable. Moreover, in all cases, low-frequency calculations must include intermolecular interactions.

An interesting aside should be noted here regarding morphology effects. The computational calculations calculate just the vibrational modes; however, many of the sample preparations may produce polycrystalline

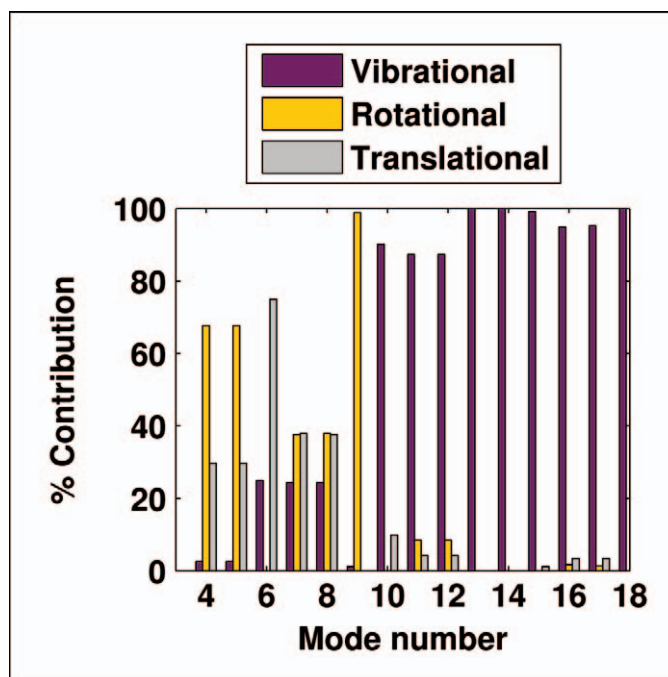


**Fig. 14.** Mode characterization for tetrapropylammonium bromide (adapted from Burnett et al.<sup>228</sup>) for the lowest 18 vibrational modes. The change in mode character from inter- to mostly intramolecular-dominated motion occurs around mode 10, which is around  $100 \text{ cm}^{-1}$  in this material.

materials that have significant effects on the measured terahertz response due to the structure of the material. Although the effects are far reduced compared to the preferred orientation effects in XRPD, nevertheless the morphology of the sample can affect the relative mixing of the various modes. Burnett et al. introduced an effective medium approximation to the calculated vibrational modes to account for particle size and shape effects.<sup>228</sup> The use of plate-like crystal shapes had the effect of slightly shifting the relative positions of the major observed terahertz features, and they found that a calculation based on a plate-like morphology associated with the 101 crystal surface most closely resembled the observed spectra. It will be interesting to follow further investigations based on these morphological effects.

**Dispersion Corrections.** The key issue in improving the predictions of the DFT approach is in improving the approximation of the exchange-correlation potential. Standard DFT-based lattice energy minimizations tend to underestimate intermolecular interactions, in particular the dispersion interaction (the London dispersion forces). Consequently, an energy-minimized unit cell often ends up being a significant fraction larger than the experimentally determined cell; in this case, the calculated intermolecular mode frequencies will be inaccurate because the intermolecular spacing is now wrong. Previously, the approach was often to artificially fix the size of the unit cell, but more recently researchers have

tried implementing parameterized atom–atom terms to model the dispersion interactions in a technique known as DFT-D. This technique was used in the recent AIE paper mentioned earlier,<sup>203</sup> and a number of researchers are actively exploring the improvements that can be made to the vibrational predictions in the terahertz region. One of the earliest parameterizations were done by Grimme,<sup>230</sup> and this is the technique most often used in recent work. King and coworkers highlighted the advantages of the DFT-D techniques in studies of (i) 1-methylthymine, 9-methyladenine, and their 1:1 cocrystal<sup>231</sup> and (ii) the pharmaceutical naproxen.<sup>232</sup> In the former study, the strength and positions of the vibrational features matched the observed terahertz features much more closely when the DFT-D technique was employed, in particular for the cocrystal, which initially had produced unfeasible imaginary frequencies for the non-DFT-D technique, indicative of a non-energy-minimum conformation in the calculation. The second study highlighted one major issue with these parameterized techniques—the choice of coupling strength. The authors found that, by optimizing the scaling correction in the DFT-D model, much better agreement could be found between experiment and theory. This process (i.e., modifying the London force corrections to improve the DFT-D model predictability) was further tested by considering molecules that are purely dispersion bound: naphthalene and durene.<sup>233</sup> Again, through modification of the scaling correction, they were able to accurately model the experimentally measured vibrations, highlighting the improved ability to account for the dispersion interaction that this technique allows.

Current efforts focus on developing a reliable method to improve the strength of the dispersion term, either through modified techniques to estimate the scaling correction<sup>234,235</sup> or through alternative parameter-free terms<sup>236,237</sup> that employ alternative correction schemes.<sup>238</sup> Currently these techniques are challenging to reliably implement in commercially available DFT packages, but given the ongoing development of the technique as well as the complicated coupling between intra- and intermolecular motions,<sup>239</sup> they will soon filter through for more mainstream use.

## APPLICATIONS

Reviews of industrial applications of terahertz spectroscopy have focused on either the applications of terahertz pulsed imaging<sup>240</sup> or the security applications of millimeter and terahertz technologies.<sup>241</sup> There have also been recent studies on the direct application of terahertz spectroscopy (as opposed to imaging) to a number of potential industrial applications.

Potential polymer applications were reviewed by Jansen et al.<sup>242</sup> and Wietzke et al.,<sup>243</sup> demonstrating uses of terahertz spectroscopy in the monitoring of compounding processes, inspection of weld joints, and birefringence analysis of fiber-reinforced components. Oil mixtures have also been investigated; it was found

that the refinements of different fractions of crude oil could be quantitatively analyzed using THz-TDS, raising the possibility of inline checks of stored petrochemicals.<sup>244</sup>

In the pharmaceutical industry, terahertz imaging applications have been very popular in measuring the thickness and distribution of polymer film-coating structures.<sup>240</sup> Moreover, in addition to the analysis of the molecular interaction between drug molecules and formulation, as outlined before, there have been a number of studies investigating the microstructure of pharmaceutical tablets using transmission spectroscopy. Starting with the simple analysis of the shape of the transmitted terahertz pulse through a tablet initial, Juuti et al. were able to demonstrate that basic information on the bulk porosity of such powder compacts can be retrieved using THz-TDS.<sup>245</sup> This was later refined by Tuonen and coworkers to account for scattering by means of effective medium theory,<sup>246,247</sup> and this was demonstrated by Ervasti et al.<sup>248</sup> and Bawuah et al.<sup>249</sup> to have sufficient sensitivity to be applied to real-world industrial samples.

Conservation and historical art uses for terahertz spectroscopy have also been an area of interest since the pioneering work of Adam et al.<sup>250</sup> For example, Bardon et al. demonstrated the use of THz-TDS to distinguish different historical black inks, depending on their compositions, such as the ratios of iron(II) sulfate and tannic or gallic acid.<sup>251</sup> Historic plastics have also been characterized, revealing that three-dimensional THz-TDS has the potential to reveal both structural and chemical information about the materials, thereby aiding in conservation efforts.<sup>252</sup>

Finally, the food industry represents yet another potential industrial application of terahertz spectroscopy, for which Gowen et al. present an excellent general introduction.<sup>253</sup> Moisture content is one obvious application area for THz-TDS, given the strong interaction of terahertz radiation with water; this has been demonstrated in a quantitative study of food wafers, where Parasoglou et al. noted a linear correlation between transmittance and water content.<sup>254</sup> More recently, the use of THz-TDS for chemical identification was demonstrated by Baek et al. in detecting the presence of melamine in food materials such as flour, milk powder, and chocolate powder.<sup>255</sup> Although they stated that the sensitivity was not high enough for the regulatory limits, the ability of THz-TDS to pass through many packaging materials made it an attractive detection tool for food monitoring. Application of more sophisticated processing algorithms may improve the sensitivity, as will the development of a robust database of terahertz spectra for dangerous contaminants.

## CONCLUSION AND OUTLOOK

The ability to use THz-TDS to measure both the amplitude and phase of the signal makes it a very attractive technique compared to conventional far-IR



spectroscopy; the terahertz spectra allow the seamless merging of dielectric loss spectra with IR spectra, hence bridge the terahertz gap in spectral analysis. In contrast, low-frequency Raman spectroscopy has the distinct advantage of having a much higher spectral band width, which makes it possible to access the vibrational response from terahertz to mid-IR frequencies in a single measurement. Given that a low-frequency Raman setup does not operate at terahertz frequencies and, hence, is not limited to diffraction at wavelengths of hundred of micrometers, a further advantage is that much smaller samples can be measured. Nevertheless, the common limitations of Raman spectroscopy in terms of fluorescence and heat transfer from the excitation laser to the sample also apply to low-frequency Raman spectroscopy.

New techniques in the generation and detection of terahertz radiation, such as the air-biased coherent-detection (ABCD) methods developed from the generation of intense terahertz pulses in air through the use of four-wave mixing techniques, have pushed terahertz band widths out to 25 THz, finally bridging the gap between low-frequency terahertz spectroscopy and traditional IR spectroscopy.<sup>256–258</sup> This greater band width is now being used in spectroscopic studies, providing crucial complementary information to the large spectral band width of low-frequency Raman spectroscopy. Such a complete picture of the vibrational landscape will help to further refine the computational techniques, thereby painting a fuller picture to understand their behavior. Furthermore, ABCD provides another route to stand-off detection at terahertz frequencies, where propagation through the atmospheric water vapor is traditionally an enormous challenge; 18 m measurement distances were reported,<sup>259</sup> which could have applications in the security industry. Not only the greater band width but also the greater power of terahertz sources will have a significant impact in the field of terahertz spectroscopy. The ability to study nonlinear effects and to excite matter in terahertz pump–terahertz probe experiments will no doubt have an enormous effect on the field as it further matures.<sup>260</sup>

1. K.D. Möller, W.G. Rothschild. *Far-Infrared Spectroscopy*. New York: Wiley-Interscience, 1971.
2. G. Chantry. *Submillimetre Spectroscopy; A Guide to the Theoretical and Experimental Physics of the Far Infrared*. New York: Academic Press, 1971.
3. H.A. Gebbie. “Fourier Transform Spectroscopy—Recollections of the Period 1955–1960”. *Infrared Phys.* 1984. 24(2-3): 105-109. doi: 10.1016/0020-0891(84)90056-3.
4. K.-E. Peiponen, J. A. Zeitler, M. Kuwata-Gonokami, Eds. *Terahertz Spectroscopy and Imaging*. Heidelberg: Springer, 2013.
5. S.L. Dexheimer. *Terahertz Spectroscopy: Principles and Applications*. Boca Raton, FL: CRC Press, 2007.
6. M. Tonouchi. “Cutting-Edge Terahertz Technology”. *Nat. Photon.* 2007. 1: 97-105.
7. Y.-S. Lee. *Principles of THz Science and Technology*. New York: Springer, 2009.
8. M. Walther, B.M. Fischer, A. Ortner, A. Bitzer, A. Thoman, H. Helm. “Chemical Sensing and Imaging with Pulsed Terahertz Radia-

- tion”. *Anal. Bioanal. Chem.* 2010. 397(3): 1009-1017. doi:10.1007/s00216-010-3672-1.
9. P.U. Jepsen, D.G. Cooke, M. Koch. “Terahertz Spectroscopy and Imaging—Modern Techniques and Applications”. *Laser Photonics Rev.* 2010. 5(1): 124-166. doi:10.1002/lpor.201000011.
10. Y.-C. Shen. “Terahertz Pulsed Spectroscopy and Imaging for Pharmaceutical Applications: A Review”. *Int. J. Pharm.* 2011. 417(1-2): 48-60. doi:10.1016/j.ijpharm.2011.01.012.
11. M. Theuer, S.S. Harsha, D. Molter, G. Torosyan, R. Beigang. “Terahertz Time-Domain Spectroscopy of Gases, Liquids, and Solids”. *ChemPhysChem.* 2011. 12(15): 2695-2705. doi:10.1002/cphc.201100158.
12. J.B. Baxter, G.W. Guglietta. “Terahertz Spectroscopy”. *Anal. Chem.* 2011. 83(12): 4342-4368. doi:10.1021/ac200907z.
13. A.I. McIntosh, B. Yang, S.M. Goldup, M. Watkinson, R.S. Donnan. “Terahertz Spectroscopy: A Powerful New Tool for the Chemical Sciences?”. *Chem. Soc. Rev.* 2012. 41: 2072-2082. doi:10.1039/c1cs15277g.
14. E. Bründermann, H.W. Hübers, M.F. Kimmitt. *Terahertz Techniques*. Heidelberg: Springer, 2012.
15. J. El Haddad, B. Bousquet, L. Canioni, P. Mounaix. “Review in Terahertz Spectral Analysis”. *TrAC, Trends Anal. Chem.* 2013. 44: 98-105. doi:10.1016/j.trac.2012.11.009.
16. M. Takahashi. “Terahertz Vibrations and Hydrogen-Bonded Networks in Crystals”. *Crystals.* 2014. 4(2): 74-103. doi:10.3390/cryst4020074.
17. J.F. Roux, F. Garet, J.L. Coutaz. “Time Domain Spectroscopy”. In: M. Perenzoni, D.J. Paul, editors. *Physics and Applications of Terahertz Radiation*. Dordrecht: Springer, 2014. Pp. 203-231.
18. M. Perenzoni, D.J. Paul, Eds. *Physics and Applications of Terahertz Radiation*. Dordrecht: Springer Netherlands, 2014.
19. F. Franks. “Protein Stability: The Value of ‘Old Literature’”. *Biophys. Chem.* 2002. 96(2-3): 117-127. doi:10.1016/S0301-4622(02)00014-5.
20. D.H. Auston. “Picosecond Optoelectronic Switching and Gating in Silicon”. *Appl. Phys. Lett.* 1975. 26: 101-103. doi:10.1063/1.88079.
21. D.H. Auston, P.R. Smith. “Generation and Detection of Millimeter Waves by Picosecond Photoconductivity”. *Appl. Phys. Lett.* 1983. 43: 631-633. doi:10.1063/1.94468.
22. D.H. Auston, K.P. Cheung, P.R. Smith. “Picosecond Photoconducting Hertzian Dipoles”. *Appl. Phys. Lett.* 1984. 45: 284-286. doi:10.1063/1.95174.
23. C. Fattering, D. Grischkowsky. “Terahertz Beams”. *Appl. Phys. Lett.* 1989. 54: 490-492.
24. P.H. Siegel. “Terahertz Pioneer: David H. Auston”. *IEEE Trans. Terahertz Sci. Technol.* 2011. 1(1): 6-8. doi:10.1109/TTHZ.2011.2151130.
25. P.H. Siegel. “Terahertz Pioneer: Daniel R. Grischkowsky, ‘We Search for Truth and Beauty’”. *IEEE T. Thz. Sci. Tech.* 2012. 2(4): 378-382. doi:10.1109/TTHZ.2012.2198216.
26. M. van Exter, C. Fattering, D.R. Grischkowsky. “Terahertz Time-Domain Spectroscopy of Water Vapor”. *Opt. Lett.* 1989. 14(20): 1128-1130.
27. D. Grischkowsky, S. Keiding, M. van Exter, C. Fattering. “Far-Infrared Time-Domain Spectroscopy with Terahertz Beams of Dielectrics and Semiconductors”. *J. Opt. Soc. Am. B.* 1990. 7(10): 2006-2015.
28. H. Harde, D. Grischkowsky. “Coherent Transients Excited by Subpicosecond Pulses of THz Radiation”. *J. Opt. Soc. Am. B.* 1991. 8(8): 1642-1651.
29. R.A. Cheville, D. Grischkowsky. “Far-Infrared Terahertz Time-Domain Spectroscopy of Flames”. *Opt. Lett.* 1995. 20(15): 1646-1648.
30. D.H. Auston, M.C. Nuss. “Electrooptical Generation and Detection of Femtosecond Electrical Transients”. *IEEE J. Quantum Elect.* 1988. 24(2): 184-197. doi:10.1109/3.114.
31. Q. Wu, X.-C. Zhang. “Free-Space Electro-Optic Sampling of Terahertz Beams”. *Appl. Phys. Lett.* 1995. 67: 3523-3525. doi:10.1063/1.114909.
32. A. Nahata, D.H. Auston, T.F. Heinz, C. Wu. “Coherent Detection of Freely Propagating Terahertz Radiation by Electro-Optic Sampling”. *Appl. Phys. Lett.* 1996. 68: 150-152. doi:10.1063/1.116130.
33. P. Jepsen, C. Winnewisser, M. Schall, V. Schyja, S. Keiding, H.

- Helm. "Detection of THz Pulses by Phase Retardation in Lithium Tantalate". *Phys. Rev. E*. 1996. 53: R3052-R3054. doi:10.1103/PhysRevE.53.R3052.
34. Q. Wu, X.-C. Zhang. "7 Terahertz Broadband GaP Electro-Optic Sensor". *Appl. Phys. Lett.* 1997. 70: 1784-1786. doi:10.1063/1.118691.
  35. L. DuVillaret, F. Garet, J. Coutaz. "A Reliable Method for Extraction of Material Parameters in Terahertz Time-Domain Spectroscopy". *IEEE J. Sel. Top. Quant.* 1996. 2(3): 739-746. doi:10.1109/2944.571775.
  36. L. DuVillaret, F. Garet, J.L. Coutaz. "Highly Precise Determination of Optical Constants and Sample Thickness in Terahertz Time-Domain Spectroscopy". *Appl. Optics*. 1999. 38(2): 409-415.
  37. E.P.J. Parrott, B.M. Fischer, L.F. Gladden, J.A. Zeitler, P.U. Jepsen. "Terahertz Spectroscopy of Crystalline and Non-Crystalline Solids". In: K.-E. Peiponen, J.A. Zeitler, M. Kuwata-Gonokami, editors. *Terahertz Spectroscopy and Imaging*. Heidelberg: Springer, 2012. Pp. 191-227.
  38. M. Bernier, F. Garet, J. Coutaz. "Precise Determination of the Refractive Index of Samples Showing Low Transmission Bands by THz Time-Domain Spectroscopy". *IEEE Trans. Terahertz. Sci. Technol.* 2013. 3(3): 295-301. doi:10.1109/TTHZ.2013.2247793.
  39. C.V. Raman, K.S. Krishnan. "A New Type of Secondary Radiation". *Nature*. 1928. 121: 501-502. doi:10.1038/121501c0.
  40. C. Moser, F. Havermeier. "Ultra-Narrow-Band Tunable Laserline Notch Filter". *Appl. Phys. B*. 2009. 95(3): 597-601. doi:10.1007/s00340-009-3447-6.
  41. P.A. Lund, O. Faursov Nielsen, E. Praestgaard. "Comparison of Depolarized Rayleigh-Wing Scattering and Far-Infrared Absorption in Molecular Liquids". *Chem. Phys.* 1978. 28(1-2): 167-173. doi:10.1016/0301-0104(78)85047-2.
  42. J. Yarwood. "Chapter 4. Spectroscopic Studies of Intermolecular Forces in Dense Phases". *Annu. Rep. Prog. Chem. C*. 1979. 76: 99-130. doi:10.1039/PC9797600099.
  43. J. Yarwood. "Chapter 7. Spectroscopic Studies of Intermolecular Forces in Dense Phases". *Annu. Rep. Prog. Chem. C*. 1982. 79: 157-197. doi:10.1039/PC9827900157.
  44. J. Yarwood. "Combined Spectroscopic Approaches to the Elucidation of Molecular Rotation in Organic Liquids—Progress and Problems". *J. Mol. Liq.* 1987. 36: 237-254. doi:10.1016/0167-7322(87)80042-9.
  45. J. Yarwood. "Spectroscopic Studies of Intermolecular Forces in Dense Phases". *Annu. Rep. Prog. Chem. C*. 1987. 84: 155-199. doi:10.1039/pc9878400155.
  46. J. Yarwood. "Chapter 4. Spectroscopic Studies of Intermolecular Forces in Dense Phases". *Annu. Rep. Prog. Chem. C*. 1990. 87: 75-118. doi:10.1039/pc9908700075.
  47. O.F. Nielsen. "Chapter 2. Low-Frequency Spectroscopic Studies of Interactions in Liquids". *Annu. Rep. Prog. Chem. C*. 1993. 90: 3-44. doi:10.1039/PC9939000003.
  48. O.F. Nielsen. "Chapter 3. Low-Frequency Spectroscopic Studies and Intermolecular Vibrational Energy Transfer in Liquids". *Annu. Rep. Prog. Chem. C*. 1997. 93: 57-100. doi:10.1039/PC9703057.
  49. C. Ronne, K. Jensby, G.K.H. Madsen, O.F. Nielsen, S.R. Keiding. "THz Time Domain Spectroscopy of Liquids". In: J.M. Chamberlain, editor. *Proc. SPIE 3828. Terahertz Spectroscopy and Applications II*. 1999. 3828: 266-275. doi:10.1117/12.361045.
  50. J.P. Poley. "Microwave Dispersion of Some Polar Liquids". *Appl. Sci. Res.* 1955. 4: 337-387. doi:10.1007/BF02316499.
  51. G.P. Johari. "Molecular Inertial Effects in Liquids: Poley Absorption, Collision-Induced Absorption, Low-Frequency Raman Spectrum and Boson Peaks". *J. Non-Cryst. Solids*. 2002. 307-310: 114-127. doi:10.1016/S0022-3093(02)01449-7.
  52. D.A. Turton, J. Hunger, A. Stoppa, A. Thoman, M. Candelaresi, G. Hefter, M. Walther, R. Buchner, K. Wynne. "Rattling the Cage: Micro- to Mesoscopic Structure in Liquids as Simple as Argon and as Complicated as Water". *J. Mol. Liq.* 2011. 159(1): 2-8. doi:10.1016/j.molliq.2010.04.005.
  53. W. Götzke. *Complex Dynamics of Glass-Forming Liquids: A Mode-Coupling Theory*. Oxford: Oxford University Press, 2008.
  54. J. Barthel, K. Bachhuber, R. Buchner, H. Hetzenauer. "Dielectric Spectra of Some Common Solvents in the Microwave Region. Water and Lower Alcohols". *Chem. Phys. Lett.* 1990. 165(4): 369-373. doi:10.1016/0009-2614(90)87204-5.
  55. J.M.G. Barthel, R. Buchner. "High Frequency Permittivity and Its Use in the Investigation of Solution Properties". *Pure Appl. Chem.* 1991. 63(10): 1473-1482. doi:10.1351/pac199163101473.
  56. F.N. Keutsch, R.J. Saykally. "Water Clusters: Untangling the Mysteries of the Liquid, One Molecule at a Time". *Proc. Natl. Acad. Sci. USA*. 2001. 98(19): 10533-10540. doi:10.1073/pnas.191266498.
  57. H. Yada, M. Nagai, K. Tanaka. "The Intermolecular Stretching Vibration Mode in Water Isotopes Investigated with Broadband Terahertz Time-Domain Spectroscopy". *Chem. Phys. Lett.* 2009. 473(4-6): 279-283. doi:10.1016/j.cplett.2009.03.075.
  58. G.W. Chantry, H.A. Gebbie. "Sub-Millimetre Wave Spectra of Polar Liquids". *Nature*. 1965. 208(163-165): 378-378. doi:10.1038/208378a0.
  59. C. Ronne, L. Thrane, P. Astrand, A. Wallqvist, K. Mikkelsen, S. Keiding. "Investigation of the Temperature Dependence of Dielectric Relaxation in Liquid Water by THz Reflection Spectroscopy and Molecular Dynamics Simulation". *J. Chem. Phys.* 1997. 107: 5319-5331. doi:10.1063/1.474242.
  60. K. Tielrooij, R.L.A. Timmer, H.J. Bakker, M. Bonn. "Structure Dynamics of the Proton in Liquid Water Probed with Terahertz Time-Domain Spectroscopy". *Phys. Rev. Lett.* 2009. 102: 198303-198304. doi:10.1103/PhysRevLett.102.198303.
  61. D. Venables, C. Schmuttenmaer. "Spectroscopy and Dynamics of Mixtures of Water with Acetone, Acetonitrile, and Methanol". *J. Chem. Phys.* 2000. 113(24): 11222-11236.
  62. H. Yada, M. Nagai, K. Tanaka. "Origin of the Fast Relaxation Component of Water and Heavy Water Revealed by Terahertz Time-Domain Attenuated Total Reflection Spectroscopy". *Chem. Phys. Lett.* 2008. 464(4-6): 166-170. doi:10.1016/j.cplett.2008.09.015.
  63. D.A. Schmidt, O. Birer, S. Funkner, B.P. Born, R. Gnanasekaran, G.W. Schwaab, D.M. Leitner, M. Havenith. "Rattling in the Cage: Ions as Probes of Sub-Picosecond Water Network Dynamics". *J. Am. Chem. Soc.* 2009. 131(51): 18512-18517. doi:10.1021/ja9083545.
  64. D. Venables, C. Schmuttenmaer. "Far-Infrared Spectra and Associated Dynamics in Acetonitrile-Water Mixtures Measured with Femtosecond THz Pulse Spectroscopy". *J. Chem. Phys.* 1998. 108: 4935-4944.
  65. P. Dutta, K. Tominaga. "Obtaining Low-Frequency Spectra of Acetone Dissolved in Cyclohexane by Terahertz Time-Domain Spectroscopy". *J. Phys. Chem. A*. 2009. 113(29): 8235-8242.
  66. P. Dutta, K. Tominaga. "Terahertz Time-Domain Spectroscopic Study of the Low-Frequency Spectra of Nitrobenzene in Alkanes". *J. Mol. Liq.* 2009. 147(1-2): 45-51. doi:10.1016/j.molliq.2008.07.018.
  67. P. Dutta, K. Tominaga. "Dependence of Low Frequency Spectra on Solute and Solvent in Solutions Studied by Terahertz Time-Domain Spectroscopy". *Mol. Phys.* 2009. 107(18): 1845-1854. doi:10.1080/00268970902744334.
  68. K.-J. Tielrooij, J. Hunger, R. Buchner, M. Bonn, H.J. Bakker. "Influence of Concentration and Temperature on the Dynamics of Water in the Hydrophobic Hydration Shell of Tetramethylurea". *J. Am. Chem. Soc.* 2010. 132(44): 15671-15678. doi:10.1021/ja106273w.
  69. Y. Yomogida, Y. Sato, K. Yamakawa, R. Nozaki, T. Mishina, J. Nakahara. "Comparative Dielectric Study of Pentanol Isomers with Terahertz Time-Domain Spectroscopy". *J. Mol. Struct.* 2010. 970(1-3): 171-176. doi:10.1016/j.molstruc.2010.03.002.
  70. Y. Yomogida, Y. Sato, R. Nozaki, T. Mishina, J. Nakahara. "Comparative Study of Boson Peak in Normal and Secondary Alcohols with Terahertz Time-Domain Spectroscopy". *Physica B*. 2010. 405(9): 2208-2212. doi:10.1016/j.physb.2010.02.010.
  71. S. Yamaguchi, K. Tominaga, S. Saito. "Intermolecular Vibrational Mode of the Benzoic Acid Dimer in Solution Observed by Terahertz Time-Domain Spectroscopy". *Phys. Chem. Chem. Phys.* 2011. 13: 14742-14749. doi:10.1039/C1CP20912D.
  72. R. Li, C. D'Agostino, J. McGregor, M.D. Mantle, J.A. Zeitler, L.F. Gladden. "Mesoscopic Structuring and Dynamics of Alcohol/Water Solutions Probed by Terahertz Time-Domain Spectroscopy and Pulsed Field Gradient Nuclear Magnetic Resonance". *J. Phys. Chem.* 2014. 118(34): 10156-10166. doi:10.1021/jp502799x.

73. H. Hirori, K. Yamashita, M. Nagai, K. Tanaka. "Attenuated Total Reflection Spectroscopy in Time Domain Using Terahertz Coherent Pulses". *Jpn. J. Appl. Phys.* 2004. 43: L1287-L1289.
74. T. Arikawa, M. Nagai, K. Tanaka. "Characterizing Hydration State in Solution Using Terahertz Time-Domain Attenuated Total Reflection Spectroscopy". *Chem. Phys. Lett.* 2008. 457(1-3): 12-17. doi:10.1016/j.cplett.2008.03.062.
75. P. Jepsen, J. Jensen, U. Møller. "Characterization of Aqueous Alcohol Solutions in Bottles with THz Reflection Spectroscopy". *Opt. Express.* 2998. 16(13): 9318-9331.
76. U. Moller, D.G. Cooke, K. Tanaka, P.U. Jepsen. "Terahertz Reflection Spectroscopy of Debye Relaxation in Polar Liquids [Invited]". *J. Opt. Soc. Am. B.* 2009. 26(9): A113-A125. doi:10.1364/JOSAB.26.00A113.
77. A.J. Baragwanath, G.P. Swift, D. Dai, A.J. Gallant, J.M. Chamberlain. "Silicon Based Microfluidic Cell for Terahertz Frequencies". *J. Appl. Phys.* 2010. 108: 013102, doi:10.1063/1.3456175.
78. U. Heugen, G. Schwaab, E. Brundermann, M. Heyden, X. Yu, D. Leitner, M. Havenith. "Solute-Induced Retardation of Water Dynamics Probed Directly by Terahertz Spectroscopy". *Proc. Natl. Acad. Sci. USA.* 2006. 103(33): 12301-12306. doi:10.1073/pnas.0604897103.
79. M. Heyden, E. Brundermann, U. Heugen, G. Niehues, D.M. Leitner, M. Havenith. "Long-Range Influence of Carbohydrates on the Solvation Dynamics of Water-Answers from Terahertz Absorption Measurements and Molecular Modeling Simulations". *J. Am. Chem. Soc.* 2008. 130(17): 5773-5779. doi:10.1021/ja00781083.
80. S. Ebbinghaus, S. Kim, M. Heyden, X. Yu, U. Heugen, M. Gruebele, D. Leitner, M. Havenith. "An Extended Dynamical Hydration Shell Around Proteins". *Proc. Natl. Acad. Sci. USA.* 2007. 104(52): 20749-20752. doi:10.1073/pnas.0709207104.
81. S. Ebbinghaus, S. Kim, M. Heyden, X. Yu, M. Gruebele, D. Leitner, M. Havenith. "Protein Sequence- and pH-Dependent Hydration Probed by Terahertz Spectroscopy". *J. Am. Chem. Soc.* 2008. 130(8): 2374-2375. doi:10.1021/ja0746520.
82. S. Ebbinghaus, K. Meister, B. Born. "Antifreeze Glycoprotein Activity Correlates with Long-Range Protein-Water Dynamics". *J. Am. Chem. Soc.* 2010. 132(35): 12210-12211.
83. S.J. Kim, B. Born, M. Havenith, M. Gruebele. "Real-Time Detection of Protein-Water Dynamics upon Protein Folding by Terahertz Absorption Spectroscopy". *Angew. Chem. Int. Edit.* 2008. 47(34): 6486-6489. doi:10.1002/anie.200802281.
84. B. Born, H. Weingartner, E. Brundermann, M. Havenith. "Solvation Dynamics of Model Peptides Probed by Terahertz Spectroscopy. Observation of the Onset of Collective Network Motions". *J. Am. Chem. Soc.* 2009. 131(10): 3752-3755. doi:doi:10.1021/ja808997y.
85. T. Ding, R. Li, J.A. Zeitler, T.L. Huber, L.F. Gladden, A.P.J. Middelberg, R.J. Falconer. "Terahertz and Far Infrared Spectroscopy of Alanine-Rich Peptides Having Variable Ellipticity". *Opt. Express.* 2010. 18(26): 27431-27444.
86. Y. Sun, Z. Zhu, S. Chen, J. Balakrishnan, D. Abbott, A.T. Ahuja, E. Pickwell-MacPherson. "Observing the Temperature Dependent Transition of the GP2 Peptide Using Terahertz Spectroscopy". *PLoS ONE.* 2012. 7: e50306. doi:10.1371/journal.pone.0050306.
87. S. Funkner, G. Niehues, D.A. Schmidt, M. Heyden, G. Schwaab, K.M. Callahan, D.J. Tobias, M. Havenith. "Watching the Low-Frequency Motions in Aqueous Salt Solutions: The Terahertz Vibrational Signatures of Hydrated Ions". *J. Am. Chem. Soc.* 2012. 134(2): 1030-1035. doi:10.1021/ja207929u.
88. Y. Sun, Y. Zhang, E. Pickwell-MacPherson. "Investigating Antibody Interactions with a Polar Liquid Using Terahertz Pulsed Spectroscopy". *Biophys. J.* 2011. 100(1): 225-231.
89. S. Funkner, M. Havenith, G. Schwaab. "Urea, a Structure Breaker? Answers from THz Absorption Spectroscopy". *J. Phys. Chem. B.* 2012. 116(45): 13374-13380. doi:10.1021/jp308699w.
90. A. Markelz, A. Roitberg, E.J. Heilweil. "Pulsed Terahertz Spectroscopy of DNA, Bovine Serum Albumin and Collagen Between 0.1 and 2.0 THz". *Chem. Phys. Lett.* 2000. 320(1-20): 42-48. doi:10.1016/S0009-2614(00)00227-X.
91. A. Markelz, S. Whitmore, J. Hillebrecht, R. Birge. "THz Time Domain Spectroscopy of Biomolecular Conformational Modes". *Phys. Med. Biol.* 2002. 47(21): 3797-3805.
92. J. Knab, J. Chen, A. Markelz. "Hydration Dependence of Conformational Dielectric Relaxation of Lysozyme". *Biophys. J.* 2006. 90(7): 2576-2581. doi:10.1529/biophysj.105.069088.
93. A.G. Markelz, J.R. Knab, J.-Y. Chen, Y. He. "Protein Dynamical Transition in Terahertz Dielectric Response". *Chem. Phys. Lett.* 2007. 442: 413-417. doi: 10.1016/j.cplett.2007.05.080.
94. Y. He, P. Ku, J. Knab, J. Chen, A. Markelz. "Protein Dynamical Transition Does Not Require Protein Structure". *Phys. Rev. Lett.* 2008. 101: 178103-178104. doi:10.1103/PhysRevLett.101.178103.
95. M. Hishida, K. Tanaka. "Long-Range Hydration Effect of Lipid Membrane Studied by Terahertz Time-Domain Spectroscopy". *Phys. Rev. Lett.* 2011. 106: 158102. doi:10.1103/PhysRevLett.106.158102.
96. M. Hishida, K. Tanaka, Y. Yamamura, K. Saito. "Cooperativity Between Water and Lipids in Lamellar to Inverted-Hexagonal Phase Transition". *J. Phys. Soc. Jpn.* 2014. 83: 044801. doi:10.7566/JPSJ.83.044801.
97. K. Ajito, Y. Ueno. "THz Chemical Imaging for Biological Applications". *IEEE Trans. Terahertz Sci. Tech.* 2011. 1(1): 293-300. doi:10.1109/TTHZ.2011.2159562.
98. R.J. Falconer, A.G. Markelz. "Terahertz Spectroscopic Analysis of Peptides and Proteins". *J. Infrared Millim. Te.* 2012. 33(10): 973-988. doi:10.1007/s10762-012-9915-9.
99. D.K. George, A.G. Markelz. "Terahertz Spectroscopy of Liquids and Biomolecules". In: K.-E. Peiponen, A. Zeitler, M. Kuwata-Gonokami, editors. *Terahertz Spectroscopy and Imaging*. Heidelberg: Springer, 2012. Pp. 229-250.
100. D. Turton, T. Harwood, A. Laphorn, E. Ellis, K. Wynne. "Ultra-broadband Terahertz Spectroscopies of Biomolecules and Water". In: M. Betz, A.Y. Elezzabi, J.-J. Song, and K.-T. Tsen, editors. *Ultrafast Phenomena and Nanophotonics XVII*. Proc. SPIE. 2013. 8623: 862303. doi:10.1117/12.2003796.
101. S. Fan, Y. He, B.S. Ung, E. Pickwell-MacPherson. "The Growth of Biomedical Terahertz Research". *J. Phys. D. Appl. Phys.* 2014. 47: 374009. doi:10.1088/0022-3727/47/37/374009.
102. A. Morresi, L. Mariani, M.R. Distefano, M.G. Giorgini. "Vibrational Relaxation Processes in Isotropic Molecular Liquids. A Critical Comparison". *J. Raman Spectrosc.* 1995. 26(3): 179-216. doi:10.1002/jrs.1250260302.
103. M.E. Gallina, P. Sassi, M. Paolantoni, A. Morresi, R.S. Cataliotti. "Vibrational Analysis of Molecular Interactions in Aqueous Glucose Solutions. Temperature and Concentration Effects". *J. Phys. Chem. B.* 2006. 110(17): 8856-8864. doi:10.1021/jp056213y.
104. M. Paolantoni, P. Sassi, A. Morresi, S. Santini. "Hydrogen Bond Dynamics and Water Structure in Glucose-Water Solutions by Depolarized Rayleigh Scattering and Low-Frequency Raman Spectroscopy". *J. Chem. Phys.* 2007. 127(2): 024504. doi:10.1063/1.2748405.
105. K. Mazur, I.A. Heisler, S.R. Meech. "Ultrafast Dynamics and Hydrogen-Bond Structure in Aqueous Solutions of Model Peptides". *J. Phys. Chem. B.* 2010. 114(32): 10684-10691. doi:10.1021/jp106423a.
106. K. Mazur, I.A. Heisler, S.R. Meech. "THz Spectra and Dynamics of Aqueous Solutions Studied by the Ultrafast Optical Kerr Effect". *J. Phys. Chem. B.* 2011. 115(11): 2563-2573. doi:10.1021/jp111764p.
107. L. Comez, L. Lupi, A. Morresi, M. Paolantoni, P. Sassi, D. Fioretto. "More Is Different: Experimental Results on the Effect of Biomolecules on the Dynamics of Hydration Water". *J. Phys. Chem. Lett.* 2013. 4(7): 1188-1192. doi:10.1021/jz400360v.
108. D.A. Turton, H.M. Senn, T. Harwood, A.J. Laphorn, E.M. Ellis, K. Wynne. "Terahertz Underdamped Vibrational Motion Governs Protein-Ligand Binding in Solution". *Nat. Commun.* 2014. 5: 3999. doi:10.1038/ncomms4999.
109. P. Lunkenheimer, A. Pimenov, M. Dressel, Y. Goncharov, R. Bohmer, A. Loidl. "Fast Dynamics of Glass-Forming Glycerol Studied by Dielectric Spectroscopy". *Phys. Rev. Lett.* 1996. 77(2): 318-321.
110. S. Kastner, M. Köhler, Y. Goncharov, P. Lunkenheimer, A. Loidl. "High-Frequency Dynamics of Type B Glass Formers Investigated by Broadband Dielectric Spectroscopy". *J. Non-Cryst. Solids.* 2011. 357: 510-514. doi:10.1016/j.jnoncrysol.2010.06.074.



111. J. Wong, C.A. Angell. *Glass: Structure by Spectroscopy*. Ann Arbor, MI: University Microfilms International, 1991.
112. P. Lunkenheimer, A. Loidl. "The Response of Disordered Matter to Electromagnetic Fields". *Phys. Rev. Lett.* 2003. 91: 207601. doi:10.1103/PhysRevLett.91.207601.
113. C.A. Angell, K.L. Ngai, G.B. McKenna, P.F. McMillan, S.W. Martin. "Relaxation in Glassforming Liquids and Amorphous Solids". *J. Appl. Phys.* 2000. 88: 3113-3157. doi:10.1063/1.1286035.
114. K. Grzybowska, M. Paluch, A. Grzybowski, Z. Wojnarowska, L. Hawelek, K. Kolodziejczyk, K.L. Ngai. "Molecular Dynamics and Physical Stability of Amorphous Anti-Inflammatory Drug: Celecoxib". *J. Phys. Chem. B.* 2010. 114(40): 12792-12801. doi:10.1021/jp1040212.
115. G.P. Johari. "Viscous Liquids and the Glass Transition. II. Secondary Relaxations in Glasses of Rigid Molecules". *J. Chem. Phys.* 1970. 53: 2372-2388. doi:10.1063/1.1674335.
116. A. Döss, M. Paluch, H. Sillescu, G. Hinze. "From Strong to Fragile Glass Formers: Secondary Relaxation in Polyalcohols". *Phys. Rev. Lett.* 2002. 88(9): 095701. doi:10.1103/PhysRevLett.88.095701.
117. U. Strom, J.R. Hendrickson, R.J. Wagner, P.C. Taylor. "Disorder-Induced Far Infrared Absorption in Amorphous Materials". *J. Chem. Phys.* 1974. 15(11-12): 1871-1875. doi:10.1016/0038-1098(74)90106-9.
118. S.N. Taraskin, S. Simdyankin, S. Elliott, J. Neilson, T. Lo. "Universal Features of Terahertz Absorption in Disordered Materials". *Phys. Rev. Lett.* 2006. 97: 055504.
119. C.J. Reid M.W. Evans. "Dielectric and Far Infrared Study of Solutions in the Glassy State from 100 Hz to 10 THz: Discovery and Characterization of the Universal  $\gamma$  Process". *J. Chem. Phys.* 1982. 76: 2576-2584.
120. W. Schirmacher, G. Ruocco, T. Scopigno. "Acoustic Attenuation in Glasses and Its Relation with the Boson Peak". *Phys. Rev. Lett.* 2007. 98: 022501. doi:10.1103/PhysRevLett.98.022501.
121. B. Rufflé, D.A. Parshin, E. Courtens, R. Vacher. "Boson Peak and Its Relation to Acoustic Attenuation in Glasses". *Phys. Rev. Lett.* 2008. 100: 015501. doi:10.1103/PhysRevLett.100.015501.
122. B. Ruta, G. Baldi, V.M. Giordano, L. Orsingher, S. Rols, F. Scarponi, G. Monaco. "Communication: High-Frequency Acoustic Excitations and Boson Peak in Glasses: A Study of Their Temperature Dependence". *J. Chem. Phys.* 2010. 133: 041101. doi:10.1063/1.3460815.
123. J. Sibik, E.Y. Shalaev, J.A. Zeitler. "Glassy Dynamics of Sorbitol Solutions at Terahertz Frequencies". *Phys. Chem. Chem. Phys.* 2013. 15(28): 11931-11942. doi:10.1039/c3cp51936h.
124. J. Sibik, S.R. Elliot, J.A. Zeitler. "Thermal Decoupling of Molecular-Relaxation Processes from the Vibrational Density of States at Terahertz Frequencies in Supercooled Hydrogen-Bonded Liquids". *J. Phys. Chem. Lett.* 2014. 5(11): 1968-1972. doi:10.1021/jz5007302.
125. M. Naftaly, R. Miles. "Terahertz Time-Domain Spectroscopy: A New Tool for the Study of Glasses in the Far Infrared". *J. Non-Cryst. Solids.* 2005. 351(40-42): 3341-3346.
126. M. Naftaly, R. Miles. "Terahertz Time-Domain Spectroscopy of Silicate Glasses and the Relationship to Material Properties". *J. Appl. Phys.* 2007. 102: 043517.
127. E.P.J. Parrott, J.A. Zeitler, G. Simon, B. Hehlen, L.F. Gladden, S.N. Taraskin, S.R. Elliott. "Atomic Charge Distribution in Sodosilicate Glasses from Terahertz Time-Domain Spectroscopy". *Phys. Rev. B.* 82: 140203. 2010. doi:10.1103/PhysRevB.82.140203.
128. M. Zalkovskij, C. Zoffmann Bisgaard, A. Novitsky, R. Malureanu, D. Savastru, A. Popescu, P. Uhd Jepsen, A.V. Lavrinenko. "Ultrabroadband Terahertz Spectroscopy of Chalcogenide Glasses". *Appl. Phys. Lett.* 2012. 100: 031901. doi:10.1063/1.3676443.
129. J.A. Zeitler, P.F. Taday, M. Pepper, T. Rades. "Relaxation and Crystallization of Amorphous Carbamazepine Studied by Terahertz Pulsed Spectroscopy". *J. Pharm. Sci.* 2007. 96(10): 2703-2709. doi:10.1002/jps.20908.
130. A.I. McIntosh, B. Yang, S.M. Goldup, M. Watkinson, R.S. Donnan. "Crystallization of Amorphous Lactose at High Humidity Studied by Terahertz Time Domain Spectroscopy". *Chem. Phys. Lett.* 2013. 558: 104-108. doi:10.1016/j.cplett.2012.12.044.
131. J. Sibik, M.J. Sargent, M. Franklin, J.A. Zeitler. "Crystallization and Phase Changes in Paracetamol from the Amorphous Solid to the Liquid Phase". *Mol. Pharm.* 2014. 11(4): 1326-1334. doi:10.1021/mp400768m.
132. S. Wietzke, C. Jansen, T. Jung, M. Reuter, B. Baudrit, M. Bastian, S. Chatterjee, M. Koch. "Terahertz Time-Domain Spectroscopy as a Tool to Monitor the Glass Transition in Polymers". *Opt. Express.* 2009. 17(21): 19006-19014.
133. M. Schadt. "Liquid Crystal Materials and Liquid Crystal Displays". *Ann. Rev. Mater. Sci.* 1997. 27: 305-379. doi:10.1146/annurev.matsci.27.1.305.
134. D. Turchinovich, P. Knobloch, G. Luessem, M. Koch. "THz Time-Domain Spectroscopy on 4-(Trans-4'-Pentylcyclohexyl)-Benzonitril". In: I.-C. Khoo, editor. *Liquid Crystals V. Proc. SPIE* 2001. 4463: 65-70. doi:10.1117/12.449955.
135. T.-R. Tsai, C.-Y. Chen, C.-L. Pan, R.-P. Pan, X.-C. Zhang. "Terahertz Time-Domain Spectroscopy Studies of the Optical Constants of the Nematic Liquid Crystal 5CB". *Appl. Opt.* 2003. 42(13): 2372-2376.
136. R.-P. Pan, C.-F. Hsieh, C.-L. Pan, C.-Y. Chen. "Temperature-Dependent Optical Constants and Birefringence of Nematic Liquid Crystal 5CB in the Terahertz Frequency Range". *J. Appl. Phys.* 2008. 103: 093523. doi:10.1063/1.2913347.
137. R. Wilk, N. Vieweg, O. Kopschinski, T. Hasek, M. Koch. "THz Spectroscopy of Liquid Crystals from the CB Family". *J. Infrared, Millimeter, Terahertz Waves.* 2009. 30: 1139-1147. doi:10.1007/s10762-009-9537-z.
138. N. Vieweg, C. Jansen, M.K. Shakfa, M. Scheller, N. Krumbholz, R. Wilk, M. Mikulics, M. Koch. "Molecular Properties of Liquid Crystals in the Terahertz Frequency Range". *Opt. Express.* 2010. 18(6): 6097-6107.
139. G.J. Evans, J.K. Moscicki. "The Poley Absorption in Liquid Crystals". *J. Mol. Liq.* 1986. 32(2): 149-160. doi:10.1016/0167-7322(86)80020-4.
140. N. Vieweg, M. Koch. "Terahertz Properties of Liquid Crystals with Negative Dielectric Anisotropy". *Appl. Opt.* 2010. 49(30): 5764-5767.
141. C.S. Yang, C.J. Lin, R.P. Pan, C.T. Que, K. Yamamoto, M. Tani, C. Pan. "The Complex Refractive Indices of the Liquid Crystal Mixture E7 in the Terahertz Frequency Range". *J. Opt. Soc. Am. B.* 2010. 27(9): 1866-1873.
142. N. Vieweg, M. Shakfa, M. Koch. "BL037: A Nematic Mixture with High Terahertz Birefringence". *Opt. Commun.* 2011. 284(7): 1887-1889. doi:10.1016/j.optcom.2010.12.061.
143. H. Park, E.P.J. Parrott, F. Fan, M. Lim, H. Han, V.G. Chigrinov, E. Pickwell-MacPherson. "Evaluating Liquid Crystal Properties for Use in Terahertz Devices". *Opt. Express.* 2012. 20(11): 11899-11905. doi:10.1364/OE.20.011899.
144. N. Vieweg, B.M. Fischer, M. Reuter, P. Kula, R. Dabrowski, M.A. Celik, G. Frenking, M. Koch, P.U. Jepsen. "Ultrabroadband Terahertz Spectroscopy of a Liquid Crystal". *Opt. Express.* 2012. 20(27): 28249-28256.
145. M. Walther, B. Fischer, M. Schall, H. Helm, P.U. Jepsen. "Far-Infrared Vibrational Spectra of All-Trans, 9-cis and 13-cis Retinal Measured by THz Time-Domain Spectroscopy". *Chem. Phys. Lett.* 2000. 332(3-4): 389-395. doi:10.1016/S0009-2614(00)01271-9.
146. M. Walther, B.M. Fischer, P.U. Jepsen. "Noncovalent Intermolecular Forces in Polycrystalline and Amorphous Saccharides in the Far Infrared". *Chem. Phys.* 2003. 288(2-3): 261-268. doi:10.1016/S0301-0104(03)00031-4.
147. C.J. Strachan, T. Rades, D.A. Newnham, K.C. Gordon, M. Pepper, P.F. Taday. "Using Terahertz Pulsed Spectroscopy to Study Crystallinity of Pharmaceutical Materials". *Chem. Phys. Lett.* 2004. 390(1-3): 20-24. doi:10.1016/j.cplett.2004.03.117.
148. C.J. Strachan, P.F. Taday, D.A. Newnham, K.C. Gordon, J.A. Zeitler, M. Pepper, T. Rades. "Using Terahertz Pulsed Spectroscopy to Quantify Pharmaceutical Polymorphism and Crystallinity". *J. Pharm. Sci.* 2005. 94(4): 837-846.
149. P.C. Upadhyaya, Y.C. Shen, A.G. Davies, E.H. Linfield. "Terahertz Time-Domain Spectroscopy of Glucose and Uric Acid". *J. Biol. Phys.* 2003. 29(2-3): 117-121.
150. P.C. Upadhyaya, Y.C. Shen, A.G. Davies, E.H. Linfield. "Far-Infrared Vibrational Modes of Polycrystalline Saccharides". *Vib. Spectrosc.* 2004. 35(1-2): 139-143. doi:10.1016/j.vibspec.2003.12.010.
151. Y. Ueno, R. Rungsawang, I. Tomita, K. Ajito. "Quantitative

- Measurements of Amino Acids by Terahertz Time-Domain Transmission Spectroscopy". *Anal. Chem.* 2006. 78(15): 5424-8. doi:10.1021/ac060520y.
152. S.E.M. Colaianni, O.F. Nielsen. "Low-Frequency Raman Spectroscopy". *J. Mol. Struct.* 1995. 347: 267-283. doi:10.1016/0022-2860(95)08550-F.
153. A.P. Ayala. "Polymorphism in Drugs Investigated by Low Wavenumber Raman Scattering". *Vib. Spectrosc.* 2007. 45(2): 112-116. doi:10.1016/j.vibspec.2007.06.004.
154. P. Ranzieri, A. Girlando, S. Tavazzi, M. Campione, L. Raimondo, I. Bilotti, A. Brillante, R.G. Della Valle, E. Venuti. "Polymorphism and Phonon Dynamics of Alpha-Quaterthiophene". *ChemPhysChem.* 2009. 10(4): 657-663. doi:10.1002/cphc.200800771.
155. M. Lamshöft, B.B. Ivanova, M. Spittler. "Chemical Identification and Determination of Sulfonamides in N-Component Solid Mixtures Within THz-Region-Solid-State Raman Spectroscopic and Mass Spectrometric Study". *Talanta.* 2011. 85(5): 2562-2575. doi:10.1016/j.talanta.2011.08.008.
156. J.T.A. Carriere, F. Havermeier, R.A. Heyler. "THz-Raman Spectroscopy for Explosives, Chemical, and Biological Detection". In: A.W. Fountain, editor. *Chemical, Biological, Radiological, Nuclear, and Explosives (CBRNE) Sensing XIV.* Proc. SPIE. 2013. 8710: 87100M. doi:10.1117/12.2018095.
157. R.A. Heyler, J.T.A. Carriere, F. Havermeier. "THz-Raman: Accessing Molecular Structure with Raman Spectroscopy for Enhanced Chemical Identification, Analysis, and Monitoring". In: M.A. Druy, R.A. Crocombe, editors. *Next-Generation Spectroscopic Technologies VI.* Proc. SPIE 8726. 2013. 8726: 87260J. doi:10.1117/12.2018136.
158. P.J. Larkin, M. Dabros, B. Sarsfield, E. Chan, J.T. Carriere, B.C. Smith. "Polymorph Characterization of Active Pharmaceutical Ingredients (APIs) Using Low-Frequency Raman Spectroscopy". *Appl. Spectrosc.* 2014. 68(7): 758-76. doi:10.1366/13-07329.
159. J.T. Carriere, F. Havermeier. "Ultra-Low Frequency Stokes and Anti-Stokes Raman Spectroscopy at 785nm with Volume Holographic Grating Filters". In: A. Mahadevan-Jansen, W. Petrich, editors. *Biomedical Vibrational Spectroscopy V: Advances in Research and Industry.* Proc. SPIE. 2012. 8219: 821905. doi: 10.1117/12.909463.
160. S. Al-Dulaimi, A. Aina, J. Burley. "Rapid Polymorph Screening of Milligram Quantities of Pharmaceutical Material Using Phonon-Mode Raman Spectroscopy". *CrystEngComm.* 2010. 12: 1038-1040. doi:10.1039/b921114b.
161. R. Vehring, J. Ivey, L. Williams, V. Joshi, S. Dwivedi, D. Lechuga-Ballesteros. "High-Sensitivity Analysis of Crystallinity in Respirable Powders Using Low Frequency Shift-Raman Spectroscopy". *Respir. Drug Deliv.* 2012. 2: 641-644.
162. M. Yamaguchi, F. Miyamaru, K. Yamamoto, M. Tani, M. Hangyo. "Terahertz Absorption Spectra of L-, D-, and dl-Alanine and Their Application to Determination of Enantiometric Composition". *Appl. Phys. Lett.* 2005. 86: 053903. doi:10.1063/1.1857080.
163. J.P. Mathieu. "Vibration Spectra and Polymorphism of Chiral Compounds". *J. Raman Spectrosc.* 1973. 1(1): 47-51. doi:10.1002/jrs.1250010104.
164. E.P.J. Parrott, J.A. Zeitler, T. Friščić, M. Pepper, W. Jones, G.M. Day, L.F. Gladden. "Testing the Sensitivity of Terahertz Spectroscopy to Changes in Molecular and Supramolecular Structure: A Study of Structurally Similar Cocrystals". *Cryst. Growth Des.* 2009. 9(3): 1452-1460. doi:10.1021/cg8008893.
165. S.P. Delaney, D. Pan, M. Galella, S.X. Yin, T.M. Korter. "Understanding the Origins of Conformational Disorder in the Crystalline Polymorphs of Irbesartan". *Cryst Growth Des.* 2012. 12(10): 5017-5024. doi:10.1021/cg300977e.
166. S.P. Delaney, T.M. Smith, T.M. Korter. "Conformation Versus Cohesion in the Relative Stabilities of Gabapentin Polymorphs". *RSC Adv.* 2013. 4: 855-864. doi:10.1039/c3ra43887b.
167. S.P. Delaney, D. Pan, S.X. Yin, T.M. Smith, T.M. Korter. "Evaluating the Roles of Conformational Strain and Cohesive Binding in Crystalline Polymorphs of Aripiprazole". *Cryst. Growth Des.* 2013. 13(7): 2943-2952. doi:10.1021/cg400358e.
168. S. Pellizzeri, S.P. Delaney, T.M. Korter, J. Zubieta. "Using Terahertz Spectroscopy and Solid-State Density Functional Theory to Characterize a New Polymorph of 5-(4-pyridyl)tetrazole". *J. Phys. Chem. A.* 2014. 118(2): 417-426. doi:10.1021/jp412142w.
169. D.V. Nickel, S.P. Delaney, H. Bian, J. Zheng, T.M. Korter, D.M. Mittleman. "Terahertz Vibrational Modes of the Rigid Crystal Phase of Succinonitrile". *J. Phys. Chem. A.* 2014. 118(13): 2442-2446. doi:10.1021/jp411865n.
170. R. Li, J.A. Zeitler, D. Tomerini, E.P.J. Parrott, L.F. Gladden, G.M. Day. "A Study into the Effect of Subtle Structural Details and Disorder on the Terahertz Spectrum of Crystalline Benzoic Acid". *Phys. Chem. Chem. Phys.* 2010. 12(20): 5329-5340. doi:10.1039/b926536h.
171. R. Rungsawang, Y. Ueno, I. Tomita, K. Ajito. "Terahertz Notch Filter Using Intermolecular Hydrogen Bonds in a Sucrose Crystal". *Opt. Express.* 2006. 14(12): 5765-5772.
172. J. Melinger, N. Laman, S. Harsha, D.R. Grischkowsky. "Line Narrowing of Terahertz Vibrational Modes for Organic Thin Polycrystalline Films Within a Parallel Plate Waveguide". *Appl. Phys. Lett.* 2006. 89: 251110. doi:251110 Artn 251110.
173. J. Melinger, N. Laman, D.R. Grischkowsky. "The Underlying Terahertz Vibrational Spectrum of Explosives Solids". *Appl. Phys. Lett.* 2008. 93: 011102-011103. doi:10.1063/1.2949068.
174. N. Laman, S.S. Harsha, D.R. Grischkowsky, J.S. Melinger. "High-Resolution Waveguide THz Spectroscopy of Biological Molecules". *Biophys. J.* 2008. 94(3): 1010-1020. doi:10.1529/biophysj.107.113647.
175. N. Laman, S.S. Harsha, D.R. Grischkowsky. "Narrow-Line Waveguide Terahertz Time-Domain Spectroscopy of Aspirin and Aspirin Precursors". *Appl. Spectrosc.* 2008. 62(3): 319-326. doi:10.1364/OL.26.000846.
176. J. Melinger, S. Harsha, N. Laman, D.R. Grischkowsky. "Guided-Wave Terahertz Spectroscopy of Molecular Solids [Invited]". *J. Opt. Soc. Am. B.* 2009. 26(9): A79-A89. doi:10.1364/JOSAB.26.000A79.
177. S.S. Harsha, J.S. Melinger, S.B. Qadri, D.R. Grischkowsky. "Substrate Independence of THz Vibrational Modes of Polycrystalline Thin Films of Molecular Solids in Waveguide THz-TDS". *J. Appl. Phys.* 2012. 111: 023105. doi:10.1063/1.3678000.
178. O. Kambara, A. Tamura, T. Uchino, K. Yamamoto, K. Tominaga. "Terahertz Time-Domain Spectroscopy of Poly-L-Lysine". *Biopolymers.* 2010. 93(8): 735-739. doi:10.1002/bip.21467.
179. H. Hoshina, Y. Morisawa, H. Sato, H. Minamide, I. Noda, Y. Ozaki, C. Otani. "Polarization and Temperature Dependent Spectra of Poly(3-Hydroxyalkanoate)s Measured at Terahertz Frequencies". *Phys. Chem. Chem. Phys.* 2011. 13: 9173-9179. doi:10.1039/C0CP02435J.
180. H. Hoshina, S. Ishii, Y. Morisawa, H. Sato, I. Noda, Y. Ozaki, C. Otani. "Isothermal Crystallization of Poly(3-Hydroxybutyrate) Studied by Terahertz Two-Dimensional Correlation Spectroscopy". *Appl. Phys. Lett.* 2012. 100: 011907. doi:10.1063/1.3673847.
181. H. Hoshina, S. Ishii, S. Yamamoto, Y. Morisawa, H. Sato, T. Uchiyama, Y. Ozaki, C. Otani. "Terahertz Spectroscopy in Polymer Research: Assignment of Intermolecular Vibrational Modes and Structural Characterization of Poly(3-Hydroxybutyrate)". *IEEE Trans. Terahertz Sci. Technol.* 2013. 3(3): 248-258. doi:10.1109/TTHZ.2013.2253154.
182. H. Hoshina, S. Ishii, H. Suzuki, C. Otani, Y. Morisawa, H. Sato, S. Yamamoto, Y. Ozaki, I. Noda. "Terahertz Vibrational Spectroscopy of Poly(3-Hydroxybutyrate) and Nylon: Potential of Terahertz Spectroscopy for Polymer Science". Paper presented at 2013 IEEE International Conference on Solid Dielectrics (ICSD). Bologna, Italy; June 30-July 4 2013. doi:10.1109/ICSD.2013.6619826.
183. S. Yamamoto, Y. Morisawa, H. Sato, H. Hoshina, Y. Ozaki. "Quantum Mechanical Interpretation of Intermolecular Vibrational Modes of Crystalline Poly-(R)-3-Hydroxybutyrate Observed in Low-Frequency Raman and Terahertz Spectra". *J. Phys. Chem. B.* 2013. 117(7): 2180-2187. doi:10.1021/jp309704k.
184. M. Tani, S. Matsuura, K. Sakai, S. Nakashima. "Emission Characteristics of Photoconductive Antennas Based on Low-Temperature-Grown GaAs and Semi-Insulating GaAs". *Appl. Opt.* 1997. 36(3): 7853-7859.

185. H. Park, E.P.J. Parrott, Z. Huang, H.P. Chan, E. Pickwell-MacPherson. "Accurate Photoconductive Antenna Characterization Using a Thin Film Polarizer". *Appl. Phys. Lett.* 2012. 101: 121108. doi:10.1063/1.4753795.
186. R. Rungsawang, Y. Ueno, I. Tomita, K. Ajito. "Angle-Dependent Terahertz Time-Domain Spectroscopy of Amino Acid Single Crystals". *J. Phys. Chem. B.* 2006. 110(42): 21259-21263. doi:10.1021/jp060492n.
187. R. Singh, D.K. George, J.B. Benedict, T.M. Korter, A.G. Markelz. "Improved Mode Assignment for Molecular Crystals Through Anisotropic Terahertz Spectroscopy". *J. Phys. Chem.* 2012. 116(42): 10359-10364. doi:10.1021/jp307288r.
188. Y. Ueno, R. Rungsawang, I. Tomita, K. Ajito. "Terahertz Time-Domain Spectra of Inter- and Intramolecular Hydrogen Bonds of Fumaric and Maleic Acids". *Chem. Lett.* 2006. 35(10): 1128-1129.
189. Y. Ueno, K. Ajito. "Terahertz Time-Domain Spectra of Aromatic Carboxylic Acids Incorporated in Nano-Sized Pores of Mesoporous Silicate". *Anal. Sci.* 2007. 23(7): 803-807.
190. H. Liu, X.-C. Zhang. "Dehydration Kinetics of d-Glucose Monohydrate Studied Using THz Time-Domain Spectroscopy". *Chem. Phys. Lett.* 2006. 429(1-3): 229-233. doi:10.1016/j.cplett.2006.07.100.
191. J. Zeitler, D. Newnham, P. Taday, C. Strachan, M. Pepper, K. Gordon, T. Rades. "Temperature Dependent Terahertz Pulsed Spectroscopy of Carbamazepine". *Thermochim. Acta.* 2005. 436(1-2): 71-77. doi:10.1016/j.tca.2005.07.006.
192. J.A. Zeitler, P.F. Taday, K.C. Gordon, M. Pepper, T. Rades. "Solid-State Transition Mechanism in Carbamazepine Polymorphs by Time-Resolved Terahertz Spectroscopy". *ChemPhysChem.* 2007. 8(13): 1924-1927. doi:10.1002/cphc.200700261.
193. T. Threlfall. "Polymorphism—Polymorph Myths and Misperceptions". *Eur. Pharm. Rev.* 2014. 19(3): 24-29.
194. J.A. Zeitler, D.A. Newnham, P.F. Taday, T.L. Threlfall, R.W. Lancaster, R.W. Berg, C.J. Strachan, M. Pepper, K.C. Gordon, T. Rades. "Characterization of Temperature-Induced Phase Transitions in Five Polymorphic Forms of Sulfathiazole by Terahertz Pulsed Spectroscopy and Differential Scanning Calorimetry". *J. Pharm. Sci.* 2006. 95(11): 2486-2498. doi:10.1002/jps.20719.
195. A. Hédoux, L. Paccou, Y. Guinet, J.-F. Willart, M. Descamps. "Using the Low-Frequency Raman Spectroscopy to Analyze the Crystallization of Amorphous Indomethacin". *Eur. J. Pharm. Sci.* 2009. 38(2): 156-164. doi:10.1016/j.ejps.2009.06.007.
196. J.B. Nanubolu, J.C. Burley. "Investigating the Recrystallization Behavior of Amorphous Paracetamol by Variable Temperature Raman Studies and Surface Raman Mapping". *Mol. Pharm.* 2012. 9(6): 1544-1558. doi:10.1021/mp300035g.
197. A. Hédoux, Y. Guinet, M. Descamps. "The Contribution of Raman Spectroscopy to the Analysis of Phase Transformations in Pharmaceutical Compounds". *Int. J. Pharm.* 2011. 417(1-2): 17-31. doi:10.1016/j.ijpharm.2011.01.031.
198. A. Hédoux, Y. Guinet, L. Paccou, F. Danède, P. Derollez. "Polymorphic Transformation of Anhydrous Caffeine upon Grinding and Hydrostatic Pressurizing Analyzed by Low-Frequency Raman Spectroscopy". *J. Pharm. Sci.* 2013. 102(1): 162-170. doi:10.1002/jps.23346.
199. H. Suzuki, H. Hoshina, C. Otani. "Kinetics of Polymorphic Transitions of Cyclohexanol Investigated by Terahertz Absorption Spectroscopy". *Cryst. Growth Des.* 2014. 14(8): 4087-4093. doi:10.1021/cg500706f.
200. M. Ge, W. Wang, H. Zhao, Z. Zhang, X. Yu, W. Li. "Characterization of Crystal Transformation in the Solid-State by Terahertz Time-Domain Spectroscopy". *Chem. Phys. Lett.* 2007. 444(4-6): 355-358. doi:10.1016/j.cplett.2007.07.028.
201. K.L. Nguyen, T. Frisčić, G.M. Day, L.F. Gladden, W. Jones. "Terahertz Time-Domain Spectroscopy and the Quantitative Monitoring of Mechanochemical Cocrystal Formation". *Nat. Mater.* 2007. 6: 206-209. doi:10.1038/nmat1848.
202. X. Liu, G. Liu, H. Zhao, Z. Zhang, Y. Wei, M. Liu, W. Wen, X. Zhou. "The Quantitative Monitoring of Mechanochemical Reaction Between Solid L-Tartaric Acid and Sodium Carbonate Monohydrate by Terahertz Spectroscopy". *J. Phys. Chem. Solids.* 2011. 72(11): 1245-1250. doi:10.1016/j.jpcs.2011.07.011.
203. E.P.J. Parrott, N.Y. Tan, R. Hu, J.A. Zeitler, B.Z. Tang, E. Pickwell-MacPherson. "Direct Evidence to Support the Restriction of Intramolecular Rotation Hypothesis for the Mechanism of Aggregation-Induced Emission: Temperature Resolved Terahertz Spectra of Tetraphenylethene". *Mater. Horiz.* 2014. 1(2): 251-258. doi:10.1039/c3mh00078h.
204. Y. Chen, H. Liu, Y. Deng, D. Schauki, M.J. Fitch, R. Osiander, C. Dodson, J.B. Spicer, M. Shur, X.-C. Zhang. "THz Spectroscopic Investigation of 2,4-Dinitrotoluene". *Chem. Phys. Lett.* 2004. 400(4-6): 357-361. doi:10.1016/j.cplett.2004.10.117.
205. L. Ning, J. Shen, S. Jinhai, L. Laishun, X. Xu, M. Lu, J. Yan. "Study on the THz Spectrum of Methamphetamine". *Opt. Express.* 2005. 13(18): 6750-6755.
206. D. Tomerini, G.M. Day. "Assignment of Vibrational Modes in Crystalline Materials". In: K.-E. Peiponen, J.A. Zeitler, M. Kuwata-Gonokami, editors. *Terahertz Spectroscopy and Imaging*. Heidelberg: Springer, 2013. Chap. 7, pp. 151-190.
207. D.G. Allis, J.A. Zeitler, P.F. Taday, T.M. Korter. "Theoretical Analysis of the Solid-State Terahertz Spectrum of the High Explosive RDX". *Chem. Phys. Lett.* 2008. 463(1-3): 84-89. doi:10.1016/j.cplett.2008.08.014.
208. P.M. Hakey, D.G. Allis, M.R. Hudson, T.M. Korter. "Density Functional Dependence in the Theoretical Analysis of the Terahertz Spectrum of the Illicit Drug MDMA (Ecstasy)". *IEEE Sens. J.* 2010. 10(3): 478-484. doi:10.1109/JSEN.2009.2038445.
209. B. Delley. "An All-Electron Numerical Method for Solving the Local Density Functional for Polyatomic Molecules". *J. Chem. Phys.* 1990. 92: 508-517. doi:10.1063/1.458452.
210. J. Izquierdo, A. Vega, L. Balbás, D. Sánchez-Portal, J. Junquera, E. Artacho, J. Soler, P. Ordejón. "Systematic Ab Initio Study of the Electronic and Magnetic Properties of Different Pure and Mixed Iron Systems". *Phys. Rev. B.* 2000. 61: 13639-13646. doi:10.1103/PhysRevB.61.13639.
211. R. Dovesi, R. Orlando, B. Civalleri, C. Roetti, V.R. Saunders, C.M. Zicovich-Wilson. "CRYSTAL: A Computational Tool for the Ab Initio Study of the Electronic Properties of Crystals". *Z. Kristallogr.* 2005. 220: 571-573. doi:10.1524/zkri.220.5.571.65065.
212. S.J. Clark, M.D. Segall, C.J. Pickard, P.J. Hasnip, M.I.J. Probert, K. Refson, M.C. Payne. "First Principles Methods Using CASTEP". *Z. Kristallogr.* 2005. 220(5-6): 567-570.
213. G. Kresse, J. Hafner. "Ab Initio Molecular Dynamics for Liquid Metals". *Phys. Rev. B.* 1993. 47: 558-561. doi:10.1103/PhysRevB.47.558.
214. D.G. Allis, D.A. Prokhorova, T.M. Korter. "Solid-State Modeling of the Terahertz Spectrum of the High Explosive HMX". *J. Phys. Chem. A.* 2006. 110(5): 1951-1959. doi:10.1021/jp0554285.
215. D.G. Allis, T.M. Korter. "Theoretical Analysis of the Terahertz Spectrum of the High Explosive PETN". *ChemPhysChem.* 2006. 7(11): 2398-2408. doi:10.1002/cphc.200600456.
216. M.D. King, P.M. Hakey, T.M. Korter. "Discrimination of Chiral Solids: A Terahertz Spectroscopic Investigation of L- and dl-Serine". *J. Phys. Chem. A.* 2010. 114(8): 2945-2953. doi:10.1021/jp911863v.
217. P.M. Hakey, D.G. Allis, W. Ouellette, T.M. Korter. "Cryogenic Terahertz Spectrum of (+)-Methamphetamine Hydrochloride and Assignment Using Solid-State Density Functional Theory". *J. Phys. Chem. A.* 2009. 113(17): 5119-5127. doi:10.1021/jp810255e.
218. P.M. Hakey, D.G. Allis, M.R. Hudson, W. Ouellette, T.M. Korter. "Terahertz Spectroscopic Investigation of S-(+)-Ketamine Hydrochloride and Vibrational Assignment by Density Functional Theory". *J. Phys. Chem. A.* 2010. 114(12): 4364-4374. doi:10.1021/jp910861m.
219. M.D. King, T.M. Korter. "Effect of Waters of Crystallization on Terahertz Spectra: Anhydrous Oxalic Acid and Its Dihydrate". *J. Phys. Chem. A.* 2010. 114(26): 7127-7138. doi:10.1021/jp101935n.
220. P.U. Jepsen, S.J. Clark. "Precise Ab-Initio Prediction of Terahertz Vibrational Modes in Crystalline Systems". *Chem. Phys. Lett.* 2007. 442(4-6): 275-280. doi:10.1016/j.cplett.2007.05.112.
221. M. Takahashi, Y. Kawazoe, Y. Ishikawa, H. Ito. "Interpretation of Temperature-Dependent Low Frequency Vibrational Spectrum of Solid-State Benzoic Acid Dimer". *Chem. Phys. Lett.* 2009. 479(4-6): 211-217. doi:10.1016/j.cplett.2009.08.017.
222. H. Yan, W.-H. Fan, Z.-P. Zheng. "Investigation on Terahertz



- Vibrational Modes of Crystalline Benzoic Acid". *Opt. Commun.* 2012. 285(6): 1593-1598. doi:10.1016/j.optcom.2011.11.046.
223. S.L. Price, D.J. Willock, M. Leslie, G.M. Day. DMAREL, Version 3.1. London: University College of London, 2001. <http://www.cse.scitech.ac.uk/ccg/software/DMAREL/> [accessed 12 Nov 2014].
  224. G.M. Day, S.L. Price, M. Leslie. "Atomistic Calculations of Phonon Frequencies and Thermodynamic Quantities for Crystals of Rigid Organic Molecules". *J. Phys. Chem. B.* 2003. 107(39): 10919-10933. doi:10.1021/jp035125f.
  225. G.M. Day, J.A. Zeitler, W. Jones, T. Rades, P.F. Taday. "Understanding the Influence of Polymorphism on Phonon Spectra: Lattice Dynamics Calculations and Terahertz Spectroscopy of Carbamazepine". *J. Phys. Chem. B.* 2006. 110(1): 447-456. doi:10.1021/jp055439y.
  226. A.D. Burnett, J. Kendrick, J.E. Cunningham, M.D. Hargreaves, T. Munshi, H.G.M. Edwards, E.H. Linfield, A.G. Davies. "Calculation and Measurement of Terahertz Active Normal Modes in Crystalline PETN". *ChemPhysChem.* 2010. 11(2): 368-378. doi:10.1002/cphc.200900548.
  227. M.R.C. Williams, A.B. True, A.F. Izmaylov, T.A. French, K. Schroeck, C.A. Schmuttenmaer. "Terahertz Spectroscopy of Enantiopure and Racemic Polycrystalline Valine". *Phys. Chem. Chem. Phys.* 2011. 13(24): 11719-11730. doi:10.1039/c1cp20594c.
  228. A.D. Burnett, J. Kendrick, C. Russell, J. Christensen, J.E. Cunningham, A.R. Pearson, E.H. Linfield, A.G. Davies. "Effect of Molecular Size and Particle Shape on the Terahertz Absorption of a Homologous Series of Tetraalkylammonium Salts". *Anal. Chem.* 2013. 85(16): 7926-7934. doi:10.1021/ac401657r.
  229. F. Zhang, O. Kambara, K. Tominaga, J.-I. Nishizawa, T. Sasaki, H.-W. Wang, M. Hayashi. "Analysis of Vibrational Spectra of Solid-State Adenine and Adenosine in the Terahertz Region". *RSC Adv.* 2014. 4: 269-278. doi:10.1039/c3ra44285c.
  230. S. Grimme. "Semiempirical GGA-Type Density Functional Constructed with a Long-Range Dispersion Correction". *J. Comput. Chem.* 2006. 27(15): 1787-1799. doi:10.1002/jcc.
  231. M.D. King, W. Ouellette, T.M. Korter. "Noncovalent Interactions in Paired DNA Nucleobases Investigated by Terahertz Spectroscopy and Solid-State Density Functional Theory". *J. Phys. Chem. A.* 2011. 115(34): 9467-9478. doi:10.1021/jp111878h.
  232. M.D. King, W.D. Buchanan, T.M. Korter. "Application of London-Type Dispersion Corrections to the Solid-State Density Functional Theory Simulation of the Terahertz Spectra of Crystalline Pharmaceuticals". *Phys. Chem. Chem. Phys.* 2011. 13(10): 4250-4259. doi:10.1039/c0cp01595d.
  233. M.D. King, T.M. Korter. "Modified Corrections for London Forces in Solid-State Density Functional Theory Calculations of Structure and Lattice Dynamics of Molecular Crystals". *J. Phys. Chem. A.* 2012. 116(25): 6927-6934. doi:10.1021/jp303746a.
  234. T.R. Juliano, M.D. King, T.M. Korter. "Evaluating London Dispersion Force Corrections in Crystalline Nitroguanidine by Terahertz Spectroscopy". *IEEE Trans. Terahertz Sci. Technol.* 2013. 3(3): 281-287. doi:10.1109/THZ.2013.2254483.
  235. T.R. Juliano, T.M. Korter. "Terahertz Vibrations of Crystalline Acyclic and Cyclic Diglycine: Benchmarks for London Force Correction Models". *J. Phys. Chem. A.* 2013. 117(40): 10504-10512. doi:10.1021/jp407112w.
  236. M. Takahashi, Y. Ishikawa, H. Ito. "The Dispersion Correction and Weak-Hydrogen-Bond Network in Low-Frequency Vibration of Solid-State Salicylic Acid". *Chem. Phys. Lett.* 2012. 531: 98-104. doi:10.1016/j.cplett.2012.02.034.
  237. M. Takahashi, Y. Ishikawa. "Translational Vibrations Between Chains of Hydrogen-Bonded Molecules in Solid-State Aspirin Form I". *Chem. Phys. Lett.* 2013. 576: 21-25. doi:10.1016/j.cplett.2013.05.026.
  238. A. Tkatchenko, M. Scheffler. "Accurate Molecular Van Der Waals Interactions from Ground-State Electron Density and Free-Atom Reference Data". *Phys. Rev. Lett.* 2009. 102: 073005. doi:10.1103/PhysRevLett.102.073005.
  239. F. Zhang, M. Hayashi, H.-W. Wang, K. Tominaga, O. Kambara, J.-i. Nishizawa, T. Sasaki. "Terahertz Spectroscopy and Solid-State Density Functional Theory Calculation of Anthracene: Effect of Dispersion Force on the Vibrational Modes". *J. Chem. Phys.* 2014. 140(17): 174509. doi:10.1063/1.4873421.
  240. J.A. Zeitler, Y.-C. Shen. "Industrial Applications of Terahertz Imaging". In: K.-E. Peiponen, A. Zeitler, M. Kuwata-Gonokami, editors. *Terahertz Spectroscopy and Imaging*. Heidelberg: Springer, 2013. Chap. 18, pp. 451-491.
  241. A. Luukanen, R. Appleby, M. Kemp, N. Salmon. "Millimeter-Wave and Terahertz Imaging in Security Applications". In: K.-E. Peiponen, A. Zeitler, M. Kuwata-Gonokami, editors. *Terahertz Spectroscopy and Imaging*. Heidelberg: Springer, 2013. Chap. 19, pp. 491-520.
  242. C. Jansen, S. Wietzke, O. Peters, M. Scheller, N. Vieweg, M. Salhi, N. Krumbholz, C. Jördens, T. Hochrein, M. Koch. "Terahertz Imaging: Applications and Perspectives". *Appl. Opt.* 2010. 49(19): E48-E57.
  243. S. Wietzke, C. Jansen, M. Reuter, T. Jung, D. Kraft, S. Chatterjee, B. Fischer, M. Koch. "Terahertz Spectroscopy on Polymers: A Review of Morphological Studies". *J. Mol. Struct.* 2011. 1006(1-3): 41-51. doi:10.1016/j.molstruc.2011.07.036.
  244. Y.-N. Li, J. Li, Z.-M. Zeng, J. Li, Z. Tian, W.-K. Wang. "Terahertz Spectroscopy for Quantifying Refined Oil Mixtures". *Appl. Opt.* 2012. 51(24): 5885-5889.
  245. M. Juuti, H. Tuononen, T. Prykäri, V. Kontturi, M. Kuosmanen, E. Alarousu, J. Ketolainen, R. Myllyl, K. Peiponen. "Optical and Terahertz Measurement Techniques for Flat-Faced Pharmaceutical Tablets: A Case Study of Gloss, Surface Roughness and Bulk Properties of Starch Acetate Tablets". *Meas. Sci. Technol.* 2009. 20(1): 015301. doi:10.1088/0957-0233/20/1/015301.
  246. H. Tuononen, E. Gornov, J.A. Zeitler, J. Aaltonen, K.E. Peiponen. "Using Modified Kramers-Kronig Relations to Test Transmission Spectra of Porous Media in THz-TDS". *Opt. Lett.* 2010. 35(5): 631-633.
  247. H. Tuononen, K. Fukunaga, M. Kuosmanen, J. Ketolainen, K.-E. Peiponen. "Wiener Bounds for Complex Permittivity in Terahertz Spectroscopy: Case Study of Two-Phase Pharmaceutical Tablets". *Appl. Spectrosc.* 2010. 64(1): 127-131.
  248. T. Ervasti, P. Silfsten, J. Ketolainen, K.-E. Peiponen. "A Study on the Resolution of a Terahertz Spectrometer for the Assessment of the Porosity of Pharmaceutical Tablets". *Appl. Spectrosc.* 2011. 66(3): 319-323. doi:10.1366/11-06315.
  249. P. Bawuah, A. Pierotic Menda, P. Silfsten, P. Pääkkönen, T. Ervasti, J. Ketolainen, J.A. Zeitler, K.-E. Peiponen. "Detection of Porosity of Pharmaceutical Compacts by Terahertz Radiation Transmission and Light Reflection Measurement Techniques". *Int. J. Pharm.* 2014. 465(1-2): 70-76. doi:10.1016/j.ijpharm.2014.02.011.
  250. A.J.L. Adam, P.C.M. Planken, S. Meloni, J. Dik. "Terahertz Imaging of Hidden Paint Layers on Canvas". *Opt. Express.* 2009. 17(5): 3407. doi:10.1364/OE.17.003407.
  251. T. Bardou, R.K. May, P.F. Taday, M. Strlič. "Systematic Study of Terahertz Time-Domain Spectra of Historically Informed Black Inks". *Analyst.* 2013. 138(17): 4859-4869. doi:10.1039/c3an00331k.
  252. G. Pastorelli, T. Trafela, P.F. Taday, A. Portieri, D. Lowe, K. Fukunaga, M. Strlič. "Characterisation of Historic Plastics Using Terahertz Time-Domain Spectroscopy and Pulsed Imaging". *Anal. Bioanal. Chem.* 2012. 403(5): 1405-1414. doi:10.1007/s00216-012-5931-9.
  253. A.A. Gowen, C. O'Sullivan, C. O'Donnell. "Terahertz Time Domain Spectroscopy and Imaging: Emerging Techniques for Food Process Monitoring and Quality Control". *Trends Food Sci. Technol.* 2012. 25(1): 40-46. doi:10.1016/j.tifs.2011.12.006.
  254. P. Parasoglou, E.P.J. Parrott, J.A. Zeitler, J. Rasburn, H. Powell, L.F. Gladden, M.L. Johns. "Quantitative Water Content Measurements in Food Wafers Using Terahertz Radiation". *Terahertz Sci. Technol.* 2010. 3(4): 172-182. doi:10.11906/TST.172-182.2010.12.17.
  255. S.H. Baek, H.B. Lim, H.S. Chun. "Detection of Melamine in Foods Using Terahertz Time-Domain Spectroscopy". *J. Agric. Food Chem.* 2014. 62(24): 5403-5407. doi:10.1021/jf501170z.
  256. D.J. Cook, R.M. Hochstrasser. "Intense Terahertz Pulses by Four-Wave Rectification in Air". *Opt. Lett.* 2000. 25(16): 1210-1212.
  257. X. Xie, J. Dai, X.-C. Zhang. "Coherent Control of THz Wave Generation in Ambient Air". *Phys. Rev. Lett.* 2006. 96(7): 075005. doi:10.1103/PhysRevLett.96.075005.

- 
258. N. Karpowicz, J. Dai, X. Lu, Y. Chen, M. Yamaguchi, H. Zhao, X.-C. Zhang, L. Zhang, C. Zhang, M. Price-Gallagher, C. Fletcher, O. Mamer, A. Lesimple, K. Johnson. "Coherent Heterodyne Time-Domain Spectrometry Covering the Entire 'Terahertz Gap'". *Appl. Phys. Lett.* 2008. 92: 011131. doi:10.1063/1.2828709.
259. J. Dai, X. Guo, X.-C. Zhang. "Terahertz Air Photonics for Standoff Explosive Detection". Paper presented at IEEE Conference on Technologies for Homeland Security, 2009 (HST '09). Boston; May 11-12 2009. doi:10.1109/THS.2009.5168073.
260. M.C. Hoffmann. "Nonlinear Terahertz Spectroscopy". In: K.-E. Peiponen, A. Zeitler, M. Kuwata-Gonokami, editors. *Terahertz Spectroscopy and Imaging*. Heidelberg: Springer, 2012. Pp. 355-388.